

1 **Title**

2 Methodological Considerations for Studying Neural Oscillations

3 *running title: analysis of neural oscillations*

4

5 **Authors**

6 Thomas Donoghue¹, Natalie Schaworonkow¹, & Bradley Voytek^{1, 2, 3, 4}

7

8 *Affiliations*

9 ¹Department of Cognitive Science, University of California, San Diego

10 ²Neurosciences Graduate Program, University of California, San Diego

11 ³Halicioğlu Data Science Institute, University of California, San Diego

12 ⁴Kavli Institute for Brain and Mind, University of California, San Diego

13

14 *Corresponding Author*

15 Thomas Donoghue: tdonoghue.research@gmail.com

16

17 *Contributions*

18 All authors contributed to designing the study. T.D and N.S did the analyses and created the figures. All
19 authors contributed to writing and editing the paper.

20

21 *ORCIDs*

22 Donoghue 0000-0001-5911-0472

23 Schaworonkow 0000-0002-2103-1178

24 Voytek 0000-0003-1640-2525

25

26 *Conflicts of Interest*

27 The authors declare no competing interests.

28

29 **Acknowledgements**

30

31 We would like to thank Ryan Hammonds for his contributions to the methods and software tools used for
32 this report. This work was supported by research funding from the National Institute of General Medical
33 Sciences grant R01GM134363-02, National Science Foundation grant BCS-1736028, and a UC San Diego
34 Halicioğlu Data Science Institute Fellowship.

35

36 **Materials Descriptions & Availability Statements**

37

38 **Project Repository**

39

40 This project is also made openly available through an online project repository in which the code
41 and data are made available, with step-by-step guides through the analyses.

42

43 Project Repository: <https://github.com/voytekresearch/OscillationMethods>

44

45 **Datasets**

46

47 This project uses simulated data. Code to recreate the exact simulations used is included in the
48 project repository.

49

50 **Software**

51

52 Code used and written for this project was written in the Python programming language ($\geq v3.7$).
53 All the code used within this project is deposited in the project repository and is made openly
54 available and licensed for reuse.

55

56 This project uses the following Python packages for simulating and analyzing neural data:

57

58 neurodsp <https://neurodsp-tools.github.io/>

59 foof <https://foof-tools.github.io/>

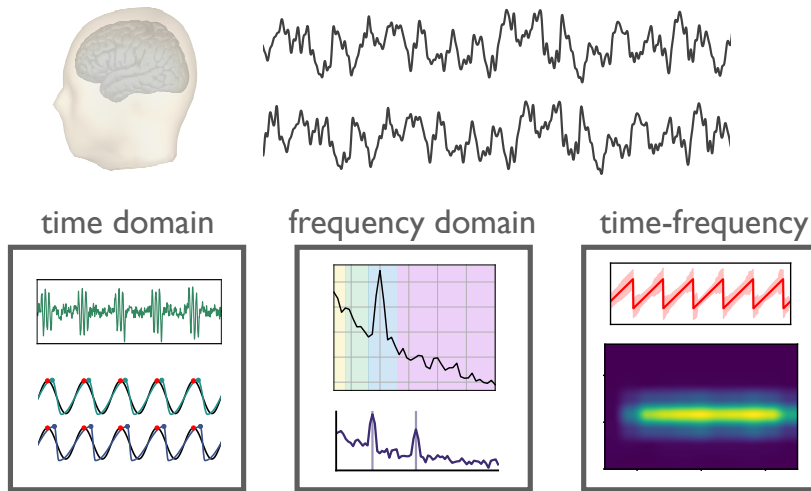
60 bycycle <https://bycycle-tools.github.io/>

61

62 In addition, third party Python toolboxes including mne, numpy, scipy, matplotlib, and seaborn
63 were used in this project.

64

methods for analyzing neural oscillations



reviewing data properties & method assumptions

65 **Graphical Abstract.** Neural oscillations are ubiquitous features of neural field data, with great potential for
66 informing our understanding of neural function and how it relates to cognition. However, there is a great
67 degree of variability in methods for investigating them, and findings that are reported. In this piece, we
68 explore methodological considerations for analyzing neural oscillations, that may underlie some potential
69 misinterpretations, and propose best practice guidelines for addressing them.

70 Abstract

71
72 Neural oscillations are ubiquitous across recording methodologies and species, broadly
73 associated with cognitive tasks, and amenable to computational modeling that investigates neural
74 circuit generating mechanisms and neural population dynamics. Because of this, neural
75 oscillations offer an exciting potential opportunity for linking theory, physiology, and mechanisms
76 of cognition. However, despite their prevalence, there are many concerns—new and old—about
77 how our analysis assumptions are violated by known properties of field potential data. For
78 investigations of neural oscillations to be properly interpreted, and ultimately developed into
79 mechanistic theories, it is necessary to carefully consider the underlying assumptions of the
80 methods we employ. Here, we discuss seven methodological considerations for analyzing neural
81 oscillations. The considerations are to 1) verify the presence of oscillations, as they may be
82 absent; 2) validate oscillation band definitions, to address variable peak frequencies; 3) account
83 for concurrent non-oscillatory aperiodic activity, which might otherwise confound measures;
84 measure and account for 4) temporal variability and 5) waveform shape of neural oscillations,
85 which are often bursty and/or nonsinusoidal, potentially leading to spurious results; 6) separate
86 spatially overlapping rhythms, which may interfere with each other; and 7) consider the required
87 signal-to-noise ratio for obtaining reliable estimates. For each topic, we provide relevant
88 examples, demonstrate potential errors of interpretation, and offer suggestions to address these
89 issues. We primarily focus on univariate measures, such as power and phase estimates, though
90 we discuss how these issues can propagate to multivariate measures. These considerations and
91 recommendations offer a helpful guide for measuring and interpreting neural oscillations.

92

93 **Keywords**

94 neural field data, digital signal processing, electrophysiology, time series analysis,
95 spectral analysis

96

97 **Abbreviations**

98 EEG: electroencephalography; MEG: magnetoencephalography; SNR: signal-to-noise ratio

99

100 Introduction

101 Recordings of electrical or magnetic fields in the brain, collectively referred to as neural
102 field recordings, are commonly used for investigating links between physiology and behavior,
103 cognition, and disease. A striking feature of such recordings is the prominent rhythmic activity,
104 termed neural oscillations (Buzsáki & Draguhn, 2004), that stands out in the otherwise seemingly
105 chaotic activity of the brain. Neural oscillations have been a feature of interest since the early
106 days of electrical brain recordings (Brazier, 1958), and are widely observed, being ubiquitously
107 present across species (Buzsáki et al., 2013). Physiologically, field potential recordings largely
108 reflect the aggregate postsynaptic and transmembrane currents of thousands to millions of
109 neurons (Buzsáki et al., 2012), with neural oscillations thought to relate to population synchrony
110 (Wang, 2010). As such, neural oscillations potentially offer insight into the coordination of neural
111 activity at the population level. Theories of the functions of oscillations argue that they facilitate
112 dynamic temporal and spatial organization of neural activity (Fries, 2005; VanRullen, 2016; Varela
113 et al., 2001; Voytek & Knight, 2015). Disruptions of oscillations have also been widely linked to
114 neurological and psychiatric disease, and have been explored as potential biomarkers of disease
115 status, drug efficacy, and other clinical indicators (Başar, 2013; Buzsáki & Watson, 2012; Newson
116 & Thiagarajan, 2019).

117 Reflecting this broad interest, thousands of investigations conducted across many
118 decades have reported associations between oscillations and just about every aspect of behavior
119 and cognition that can be operationalized (Başar et al., 2001; Lopes da Silva, 2013; Mazaheri et
120 al., 2018). As neural oscillations appear at many different temporal scales (Buzsáki et al., 2013),
121 investigations often focus on predefined canonical frequency band ranges that are thought to
122 capture distinct oscillations. For example, sleep researchers often study delta (1-4 Hz), memory
123 researchers theta (4-8 Hz), visual researchers alpha (8-12 Hz), and cognitive and motor
124 researchers beta (13-30 Hz) frequency bands. In doing so, research in neural oscillations spans
125 across different recording modalities (Buzsáki et al., 2012)—including both non-invasive and
126 invasive methods—and across different brain regions (Frauscher et al., 2018; Mahjoory et al.,
127 2020).

128 While oscillations provide an exciting possibility to link cognition and disease to theory and
129 physiology, there are often inconsistent reports regarding which oscillations are modulated by
130 which conditions and how. In part, this likely reflects the variety of approaches taken, with limited
131 consistency in terms of experimental design, analysis methods, parameter choices, and
132 theoretical frameworks used across studies. Open challenges include developing more consistent

133 terminology and interpretations (Cohen & Gulbinaite, 2014), and the need for explicitly
134 considering replicability in electrophysiological investigations (Cohen, 2017a). Accordingly, best
135 practice guidelines for research (Gross et al., 2013; Keil et al., 2014; Pernet et al., 2020; Pesaran
136 et al., 2018) and clinical investigations (Babiloni et al., 2020) have been proposed to improve
137 standards of reporting, and therefore reproducibility, for research using neural field recordings.

138 As an extension of these general guidelines, here we examine common interpretational
139 considerations in analyzing neural field recordings. Given the advances in both methods
140 development and our understanding of the empirical properties of the data under study, it is
141 critically important to ensure that common analysis methods are appropriately applied, as this is
142 a core requisite for accurate interpretation. There is a large toolkit of analysis methods for studying
143 neural oscillations, across both the spectral and temporal domains, borrowed and adapted from
144 the field of digital signal processing. These methods are described and compared in other work
145 focused on methodological properties of particular estimation techniques (Bruns, 2004; Gross,
146 2014; van Vugt et al., 2007; Wacker & Witte, 2013).

147 Here, we focus more explicitly on properties of neural oscillations, and how these
148 properties relate to commonly applied methods, rather than focus on the methods themselves.
149 We address how common analysis approaches can give rise to results that are easy for
150 researchers to misinterpret, due to the misalignment between methodological or experimental
151 assumptions, and properties of the data. As such, these considerations are not restricted to
152 individual estimators (such as using particular filters, or a particular estimate of power), as they
153 reflect more general properties of signal processing methods and neural data. Importantly, these
154 are not failures of the algorithms per se, which do, mathematically, exactly what they should; the
155 potential pitfalls lay in how we interpret their outputs. If and when there is a misalignment between
156 methodological assumptions and data properties, computed measures can lack validity which can
157 lead to inconsistent results. This in turn impedes us from properly grounding oscillation research
158 in physiology and theory.

159 To address these issues, we examine common interpretational considerations in studying
160 neural oscillations, in order to identify and address possible methodological concerns that may
161 lead to interpretation errors. We consider recurring themes based on our developing
162 understanding of neural field data, and how this understanding relates to the application of
163 analysis methods. For example, a common assumption is that neural field data can be quantified
164 as a series of oscillatory signals, often assumed to be stationary. However, in empirical
165 neurophysiological data, oscillations show large variability in their presence and extent across
166 time, as well as across participants and cortical regions (Donoghue et al., 2020b; Frauscher et

167 al., 2018; Groppe et al., 2013). Even when oscillations are present, they are highly variable
168 (Jones, 2016; Neymotin, Barczak, et al., 2020), waxing and waning in short bursts and including
169 longer, more tonic rhythms, with rapidly changing amplitude, frequency, and phase dynamics that
170 are not easily captured by common analyses and predefined canonical frequency ranges. This
171 potentially meaningful variation of cycle features across time can be blurred by narrowband
172 filtering (de Cheveigné & Nelken, 2019) and lead to misinterpretations of which features of the
173 oscillation have truly changed (Cole & Voytek, 2019). All of these properties, and more, need to
174 be explicitly considered in order to accurately and reliably measure oscillatory neural activity.

175 We organize methodological considerations for analyzing neural oscillations into seven
176 areas, each with example demonstrations (see **Box 1**). The primary focus is on univariate
177 measures of oscillatory power, frequency, and phase, including potential pitfalls and
178 considerations for ensuring accurate measurement and interpretation of these aspects, as well
179 as discussions of how these issues can propagate to multivariate analyses, such as cross-
180 frequency coupling. These demonstrations make use of simulated data, which is created to match
181 known properties of neural field recordings whereby key features of the simulated neural field
182 activity were chosen and manipulated to reflect experimentally observed variations in empirical
183 data. We analyze the simulated data using common spectral and time-domain analysis methods
184 in order to evaluate their performance in relation to the interplay of data properties and method
185 assumptions. Each consideration is then contextualized within the broader literature, and specific
186 practical recommendations are made to help guide the analysis of neural oscillations. The
187 simulated data and analysis methods were created and used from the NeuroDSP module (Cole
188 et al., 2019), with all associated code for recreating and further exploring the illustrations openly
189 available in the project repository (<https://github.com/voytekresearch/oscillationmethods>).

190

191 **Box 1:** Overview of methodological considerations for measuring neural oscillations

Topic	Data Properties	Methodological Issues	Recommendation
#1 Oscillation Presence	neural oscillations are variably present, and may not be present in the recording	if there are no oscillations, applied measures won't reflect oscillatory activity, but will return a value reflecting aperiodic activity	verify the presence of an oscillation, such as with spectral peak detection or with burst detection in the time domain
#2 Frequency Variation	neural oscillations have variable peak frequencies	measures applied using canonically defined frequency bands may fail to accurately capture oscillatory activity	verify frequency ranges and individualize as needed
#3 Aperiodic Activity	neural oscillations co-exist with dynamic aperiodic activity	measured variation may arise due to changes in aperiodic activity, rather than changes in oscillations	measure and control for changes in aperiodic neural activity, evaluating whether it explains measured changes
#4 Temporal Variability	neural oscillations are variable across time, exhibiting burst-like properties	burst properties may be conflated when analyzing spectral power, and trial averages may suggest illusory sustained activity	examine single trial data for temporal variation, and use burst detection to evaluate burst properties
#5 Waveform Shape	neural oscillations have non-sinusoidal waveform shape	analysis methods often assume sinusoidal structure, and may return spurious results in the case of non-sinusoidal oscillations	examine waveform shape measures to evaluate if waveform shape may underlie the results
#6 Overlapping Oscillations	multiple neural oscillations co-exist across the brain, and may overlap across space	multiple distinct sources may create destructive interference, in which case measures won't accurately reflect underlying activity	apply source separation techniques in order to reduce overlap of different types of oscillations
#7: Signal-to- Noise Ratio	neural oscillations have variable signal-to-noise ratio	without adequate signal to noise ratio, measures may be unreliable or inaccurate	evaluate the required signal-to-noise ratio, and potential ways to optimize it for all applied measures

193 #1 Neural oscillations are not always present

194 Why this matters

195 Neural field recordings are characterized not only by oscillatory activity, but also aperiodic
196 '1/f' or '1/f-like' activity, in which signal power decreases exponentially as a function of frequency
197 (Freeman et al., 2003; B. J. He, 2014). This is usually formalized as $1/f^\chi$ where χ represents the
198 decay of power across frequencies. In neural data, χ often ranges between 0 and 4, where a
199 signal with $\chi=0$ is white noise, with equal power across all frequencies, and higher values of χ
200 indicate increasingly 'steeper' spectra. Aperiodic neural activity has been linked to the underlying
201 activity of postsynaptic potentials and is a ubiquitous and sometimes dominant feature of neural
202 field data (Gao et al., 2017; K. J. Miller et al., 2009).

203 The fact that aperiodic activity is omnipresent together with the large observable variability
204 of neural oscillations (Donoghue et al., 2020b; Frauscher et al., 2018; Groppe et al., 2013)
205 requires care in how band-limited power obtained by spectral analysis is measured and
206 interpreted. Due to the presence of aperiodic activity, there is always non-zero power at all
207 frequency bands. This means that any spectral measure—including computing a power spectrum,
208 narrowband filtering, and average band-power measures—will always return a numerical value
209 for power for a given frequency band, even if there is no oscillatory activity present. That is, just
210 because there is power in a *frequency band* does not imply that there is an *oscillation* in that same
211 frequency band (Bullock et al., 2003). It is a fallacy to presume that an analysis of a predefined
212 narrowband frequency range necessarily reflects physiological oscillatory activity.

213 To introduce how transient and aperiodic signals are represented in the spectral domain,
214 the Dirac delta can be used, whereby a single non-zero value in the time domain is represented
215 by constant power across all frequencies in the frequency domain (Fig. 1A). This illustrates that
216 power in a specific frequency band does not generally correspond to a present oscillation in the
217 time domain. Similarly, 1/f-like aperiodic activity, which is common in neural data, shows power
218 across all frequencies, with decreasing power for higher frequencies (Fig. 1B). Despite the lack
219 of periodic activity in aperiodic time series, narrowband filtering, which imposes a sinusoidal basis,
220 extracts components that appear to be oscillatory, when filtered into canonical band ranges (Fig.
221 1C). By comparison, rhythmic signals, such as a pure sinusoid, exhibit as a frequency specific
222 peak in the power spectrum (Fig. 1D). Neural field recordings can be simulated as a summation
223 of oscillatory and aperiodic components, resulting in a power spectrum that exhibits a spectral
224 peak exceeding the aperiodic component, reflecting a high amount of band-specific power (Fig.

225 1E). In this case, the presence of the spectral peak is indicative of oscillatory power. In general,
226 since different signal components can contribute to spectral power across different frequency
227 ranges, power in a frequency band may not reflect oscillatory activity.

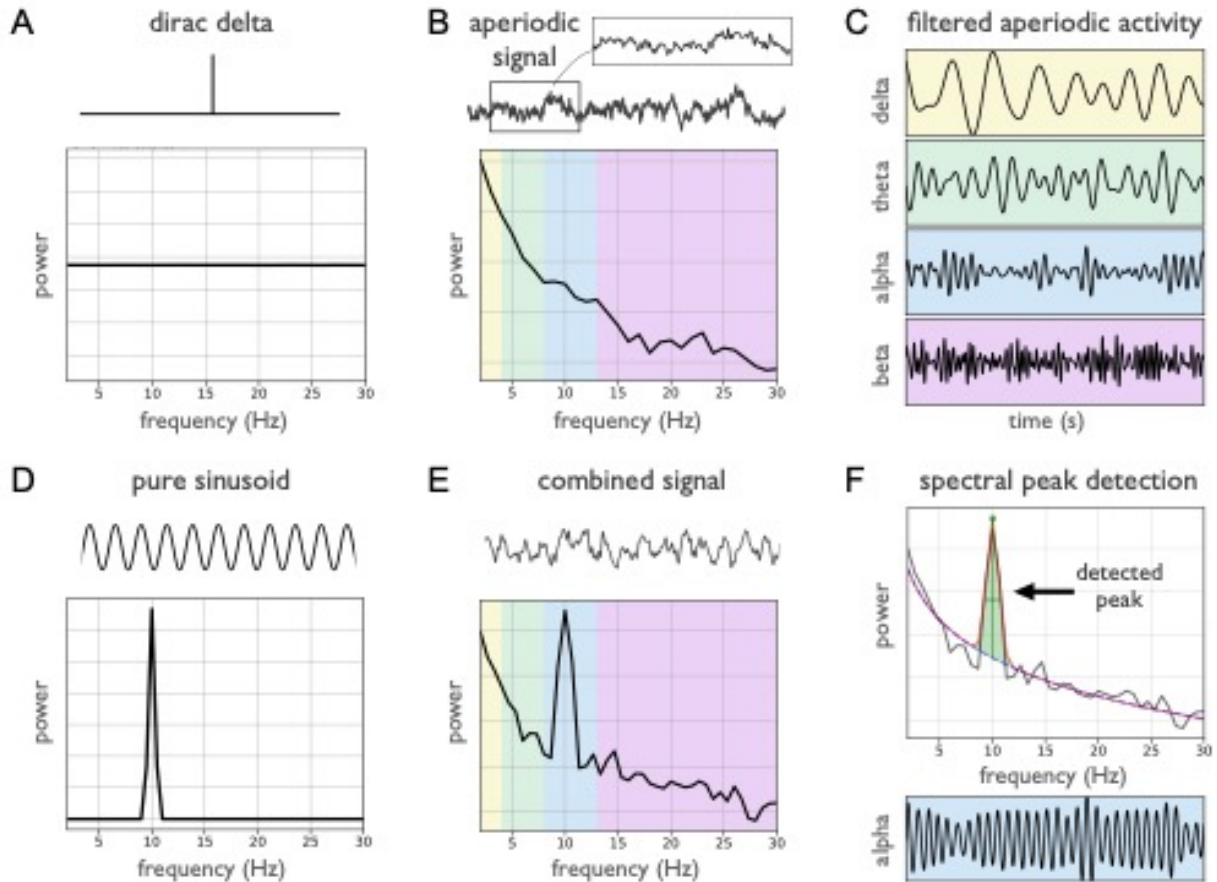
228 Recommendations

229 Investigations of oscillations should start with a *detection* step, verifying the presence of
230 oscillations of interest. This verification step can be done in both the frequency and time domains.
231 In the time domain, visualizing the data allows for examining if there are clear rhythmic segments
232 in the data. In the frequency domain, oscillations manifest as peaks of power over and above the
233 aperiodic signal (Buzsáki et al., 2013). As an initial check, visually inspecting power spectra can
234 help to verify the presence of prominent oscillations. Including figures of power spectra in
235 manuscripts is recommended, as it provides supporting evidence to the reader that there is
236 oscillatory activity in the data under study.

237 Numerous quantitative methods also exist to detect oscillatory activity in neural field data,
238 such as automated methods that detect narrowband spectral peaks (Pascual-Marqui et al., 1988).
239 This can be systematically done by parameterizing the power spectrum, in which a mathematical
240 model that quantifies periodic and aperiodic activity is applied to detect any putative oscillatory
241 peaks above the measured aperiodic component (Donoghue et al., 2020b) (see Fig. 1F).
242 Similarly, both the ‘multiple oscillation detection algorithm’ (MODAL) method (Watrous et al.,
243 2018) and the ‘extended better oscillation detection’ (eBOSC) method (Kosciessa et al., 2020),
244 which is itself an extension of prior methods (Caplan et al., 2015; Whitten et al., 2011), use a fit
245 of the aperiodic activity to detect frequency specific activity.

246 It may also be useful to examine rhythmic properties of the data, to search for putative
247 oscillatory activity in situations in which a spectral peak may be difficult to observe (Pesaran et
248 al., 2018). For example, oscillations may be present in the form of rare or infrequent bursts, which
249 will not appear as clear spectral peaks when the spectrum is calculated across the whole time
250 interval. In such situations, examining shorter time ranges, and selecting time windows with higher
251 band power and/or around events of interest may be required to resolve peaks in the frequency
252 domain. Alternatively, time domain and burst detection methods, further described in sections 4
253 and 5, may be more applicable. Another potential approach for addressing this is lagged
254 coherence (Fransen et al., 2015), which explicitly quantifies the rhythmicity in time series, in
255 contrast to measuring solely spectral power, and can also be used to differentiate between
256 oscillatory signals and transients (see Fig. 1A).

257 Because oscillations can vary in their presence within and between participants, and
258 across different frequency bands (Donoghue et al., 2020b; Frauscher et al., 2018) oscillation
259 detection should be performed for each frequency band of interest, participant and analyzed
260 region. If oscillations are not detected, this may preclude further analyses. Group-level analyses
261 may obscure variation in oscillatory presence in individual participants. For example, if not all
262 participants display a clear rhythm, effect size estimates of oscillatory changes at the group level
263 may be confounded by including the subset of participants without any clear oscillatory activity.
264 Alternatively, a comparison of oscillatory power between regions without doing oscillation
265 detection may conflate a change in oscillatory power with a difference in oscillatory presence.
266 Analyses that include filtering or band-specific measures without first examining if an oscillation
267 is present can provide ambiguous results that may reflect aperiodic activity, in which case it is a
268 misinterpretation to describe physiological *oscillatory* activity. Applying analyses to detect
269 oscillatory presence can assure that measures reflect oscillatory activity.
270



271

272 **Figure 1: Without verified oscillatory activity, applied measures may reflect aperiodic activity. A)**

273 Non-oscillatory signals such as the dirac delta function exhibit power across all frequencies. **B)** Similarly, a

274 non-oscillatory $1/f$ signal also has power across all frequencies, including canonical narrowband regions:

275 delta (yellow), theta (green), alpha (blue), and beta (purple). This power spectrum illustrates the fact that

276 just because there is power at a frequency, that does not imply there is a dominant oscillation at that

277 frequency. **C)** Narrowband filtered traces of the signal shown in B, that appear to be rhythmic. Note that

278 this reflects band-power from the aperiodic activity, rather than any narrowband oscillation. **D)** Rhythmic

279 signals, such as a pure sinusoid, exhibit as a dominant peak in the power spectrum. **E)** A combined signal

280 that contains aperiodic activity and a narrowband alpha oscillation. In this case, the oscillation is visible as

281 a peak in the power spectrum above the spectral contribution from the aperiodic $1/f$ -like signal. **F)** Spectral

282 peaks can be detected in order to identify putative oscillations in the data, as shown by the identified peak,

283 in green. Spectral peak detection can be used to select frequency bands for further analysis, for example

284 selecting the alpha range to be filtered for subsequent analysis (bottom).

285 #2 Neural oscillations vary in their peak frequencies

286 Why this matters

287 Neural oscillations display significant variations in their peak frequencies, including
288 variation across age (Lindsley, 1939), within and between participants (Haegens et al., 2014),
289 and across cortical locations (Mahjoory et al., 2020). Alpha peak frequency, for example, is
290 considered a stable trait marker (Grandy et al., 2013), and is also associated with some clinical
291 disorders, displaying, for example, a slower frequency in attention-deficit hyperactivity disorder
292 (ADHD) (Lansbergen et al., 2011). The frequency of neural oscillations can also vary within
293 participants within a task (Benwell et al., 2019), including in task relevant ways (Wutz et al., 2018).

294 Due to frequency variation, even if the presence of oscillations is verified, the use of
295 canonically defined frequency ranges may still fail to accurately reflect the data, as this may
296 misestimate power of an oscillation if the spectral peak is not well captured in the canonical range.
297 For example, in Figure 2, a canonically defined alpha range of 8-12 Hz captures the peak of a 10
298 Hz oscillation (Fig. 2A), but fails to accurately capture a 8 Hz peak (Fig. 2B). Despite the signals
299 being simulated with the same amount of oscillatory power, estimated alpha power using a
300 canonical frequency range differs between the signals (Fig. 2C), due to an underestimate of the
301 power in the signal with an idiosyncratic peak frequency. This issue also impacts the result of
302 band-pass filtering, as a canonical filter range underestimates the amount of alpha power present,
303 as compared to an individualized band in which the filter range is made to reflect the oscillation
304 in the data (Fig. 2D). Using individualized frequency band ranges to control for frequency
305 differences accurately captures the alpha power in each signal (Fig. 2E). Overall, predefined
306 frequency band definitions may fail to address variation in peak frequencies, and lead to
307 misestimations.

308 Potential differences in peak frequency are important for analyses that compute an
309 estimate within a specific frequency range, such as calculating band power, or narrowband
310 filtering to a frequency range of interest. Applying a fixed frequency range may lead to information
311 loss when the individual peak frequency lies near the border or outside of the defined range; it
312 can also be non-specific if the range captures an adjacent oscillation or aperiodic activity. These
313 issues apply both to analyses of individual frequency bands, as well as to composite measures
314 such as ratios computed between the power of different frequency bands, since variation in the
315 peak frequency or bandwidth of peaks can impact measured results (Donoghue et al., 2020a).
316 For example, what had previously been reported as a difference in the theta / beta ratio of

317 participants with ADHD was found to be partially driven by a slowed alpha peak in the ADHD
318 group, changing the interpretation of the data (Lansbergen et al., 2011).

319 Recommendations

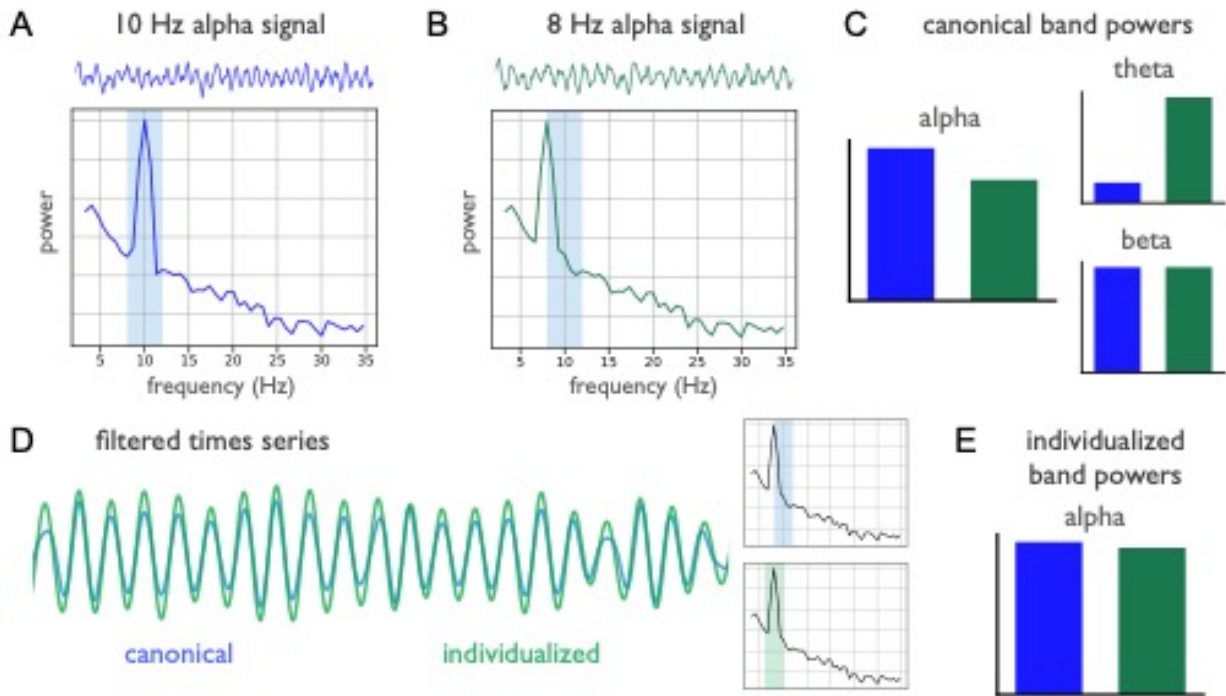
320 In order to address the variability of peak frequencies, any analyses that employ
321 narrowband frequency ranges should assess how well the chosen ranges match the data. Visual
322 inspection can help determine how well the defined frequency boundaries reflect actual peaks in
323 the power spectra. This should be done for all analyzed frequency bands at the level of individual
324 participants, because individual participants may have idiosyncratic peak frequencies that could
325 influence group level results if they are misestimated. For within-subject analyses, changes in
326 peak frequency over time or between tasks should also be considered in order to address whether
327 a measured change in power could reflect a change in peak frequency, in which frequencies may
328 'drift' outside defined ranges of interest. Including power spectra in manuscripts also enables
329 readers to observe that applied band ranges match the peaks observed in the data.

330 If canonically defined frequency ranges do appropriately match the data, then they can
331 safely be used for subsequent analyses. However, if chosen band ranges of interest do not
332 appropriately reflect the data, then individualized frequency bands may be applied (Klimesch,
333 1999). Methods for computing individualized frequency bands often do so by measuring spectral
334 peaks (Haegens et al., 2014; Pascual-Marqui et al., 1988). Automated approaches have also
335 been developed, that include spectral smoothing to improve performance (Corcoran et al., 2018).
336 Such approaches don't always generalize to multiple peaks or bands, though some approaches
337 use 'anchor frequencies' (Klimesch, 1999), defining, for example, theta as a range below the
338 identified range of alpha. This approach has the limitation of not considering the oscillation
339 detection step. Peak detection for multiple putative peaks, without predefining frequency ranges,
340 can also be done with spectral parameterization (Donoghue et al., 2020b), after which peaks can
341 be grouped into observed bands of interest.

342 Beyond spectral peak detection, methods for detecting oscillations can be used to detect
343 frequencies with peak rhythmicity, for example, by applying lagged coherence across frequencies
344 (Fransen et al., 2015). Some methods also allow for jointly learning multiple band definitions. For
345 example, the Oscillation ReConstruction Algorithm (ORCA) evaluates multiple band definitions in
346 terms of how well each definition is able to reconstruct the data (Watrous & Buchanan, 2020),
347 and the gedBounds method identifies frequency boundaries by clustering similarities across
348 frequencies (Cohen, 2021). These methods, which examine all analyzed frequencies together,
349 may help to obtain more consistent groups of frequency ranges within and across participants.

Oscillation Methods

350 Collectively, some form of evaluation needs to be done to verify frequency bands, in order to
351 ensure that applied measures accurately capture the intended oscillatory activity.
352



353 **Figure 2: Canonical frequency band ranges may fail to capture narrowband peaks.** **A)** A simulated
 354 signal, and corresponding power spectrum, with a prominent 10 Hz alpha oscillation. Shaded in blue is the
 355 canonical alpha range (8-12 Hz). **B)** Another signal with a prominent alpha oscillation, with a peak frequency
 356 of 8 Hz. **C)** Using canonical band ranges, the amount of alpha power is found to be significantly different
 357 between the signals from A & B. When examining adjacent frequency bands, (right), there is also a
 358 measured difference in theta power, due to the alpha peak drifting into the canonical theta range. These
 359 results suggest differences in oscillatory power between signals, however this is actually driven by a
 360 difference in alpha peak frequency. **D)** The time series from B, filtered into the alpha frequency range, using
 361 both the canonical range (blue) and an individualized range (green). The individualized range is tuned to
 362 the peak frequency of the time series (see inset power spectra). Note that the individualized filter captures
 363 more narrowband activity. **E)** Using individualized frequency bands, a difference in measured alpha power
 364 is no longer seen, consistent with the measured difference in C being due to a mismatch in peak frequency.

365 #3 Neural oscillations coexist with aperiodic activity

366 Why this matters

367 As previously introduced, neural field recordings contain aperiodic activity (B. J. He, 2014).
368 This activity is not only ubiquitously present, but is also variable and dynamic within and between
369 subjects (Freeman & Zhai, 2009; Podvalny et al., 2015). Between subject variability of aperiodic
370 activity can relate to age (W. He et al., 2019; Voytek et al., 2015), and clinical diagnoses
371 (Robertson et al., 2019), whereas within subjects, aperiodic activity varies with state, such as
372 sleep (Lendner et al., 2020), relates to behavioral tasks (Podvalny et al., 2015) and can be
373 influenced by exogenous stimuli and cognitive demands (Waschke et al., 2021). This dynamic
374 aperiodic activity has different putative generators, physiological interpretations, and task related
375 dynamics (Gao et al., 2017, 2020; K. J. Miller et al., 2009, 2014), as compared to oscillations,
376 making it an interesting feature of interest in itself. Altogether, aperiodic neural activity is dynamic
377 in many contexts in which neural oscillations are usually the focus of inquiry.

378 This dynamic quality of aperiodic activity is an important consideration for detecting neural
379 oscillations, as previously discussed (see #1), as well as for interpreting measured changes in
380 the data. With multiple dynamic components, analyses must adjudicate which aspects of the data
381 are changing, and how, in order to allow for appropriate interpretations. Since aperiodic activity
382 has power at all frequencies, changes or differences in aperiodic activity can induce patterns of
383 differential activity across all frequencies. This can be seen by comparing white ($\chi = 0$) and pink
384 ($\chi = 1$) noise $1/f^\chi$ signals, which have different amounts of power in a canonically defined alpha-
385 band (Fig. 3A). Even with a validated spectral peak and frequency range, a difference in band-
386 power between two conditions within a given frequency range may not be specific to oscillatory
387 changes, as it may reflect a global change in aperiodic activity. For example, in Fig. 3B, a
388 measured difference in alpha-band power between two conditions reflects a change in the
389 aperiodic exponent, not changes relating to a spectral peak in the alpha-band, since the periodic
390 activity is the same in the two signals.

391 Considering aperiodic activity is particularly important for analyses that investigate band-
392 power across a series of frequency bands, since systematic patterns of measured changes across
393 bands may not reflect any changes in oscillatory activity. For example, in Fig. 3C, the band-power
394 of two conditions is compared across five different frequency bands. Despite this analysis
395 suggesting a pattern of changes in band power across a series of canonically defined frequency
396 bands (Fig. 3D), the changes are actually driven by a change in aperiodic activity. Patterns of

397 correlated changes across frequency bands can therefore sometimes be more parsimoniously
398 explained by a change in aperiodic activity, rather than as multiple distinct oscillatory changes, as
399 has been shown to be the case in development (W. He et al., 2019).

400 Changes in global power, due to aperiodic changes, can also impact relative or normalized
401 measures of oscillatory activity. In the spectra in Fig. 3C, there is a visible spectral peak in the
402 alpha-band. Even though there is no change in peak power, a relative power measure suggests
403 a change in alpha power, due to a change in the power across all frequencies, that is driven by a
404 change in aperiodic activity (Fig. 3E). This issue also impacts other compound measures, such
405 as ratios of band-power, including the theta/beta-ratio, often investigated as a potential biomarker
406 for ADHD (Lansbergen et al., 2011; Robertson et al., 2019), as it has been shown that band ratio
407 measures often reflect a change of the aperiodic activity (Donoghue et al., 2020a), and that the
408 putative relationship between ADHD and theta/beta-ratio appears to be driven by aperiodic
409 activity (Robertson et al., 2019).

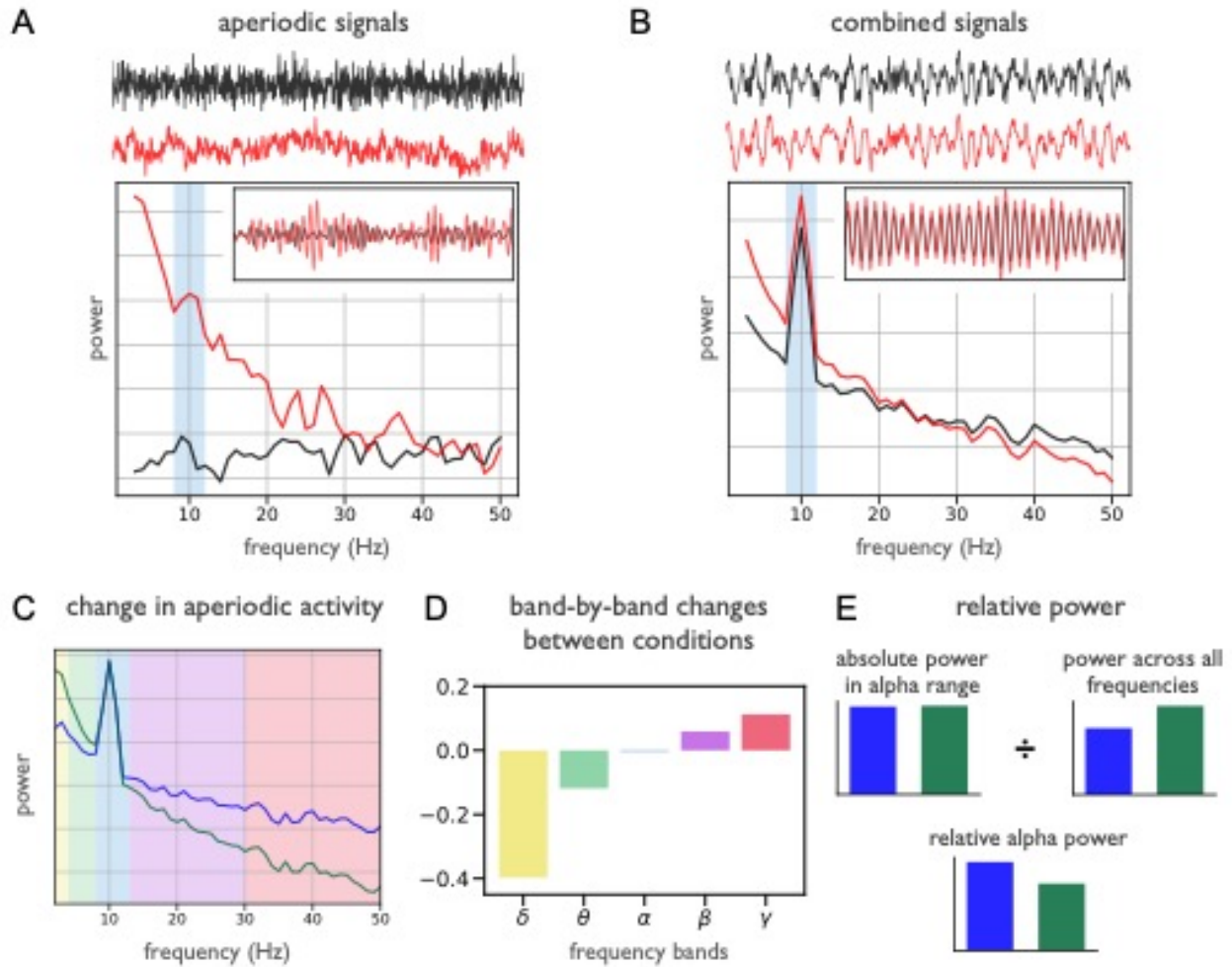
410 Recommendations

411 As both oscillatory and aperiodic components are dynamic, it is important for analyses to
412 validate which elements of the data are specifically changing, in order to appropriately interpret
413 results. This is relevant for any analysis investigating putative narrowband power, including
414 investigations that examine multiple oscillation bands. Aperiodic activity should be explicitly
415 measured to evaluate whether it explains the band-specific changes, including whether correlated
416 patterns of changes across frequency bands may be more parsimoniously explained as a change
417 in the broadband aperiodic activity. Approaches that assume oscillations exist upon a stationary
418 'background', such as relative power measures that divide by power across all frequencies, or
419 band ratio measures, should be avoided, as they conflate changes in oscillatory and aperiodic
420 components (Donoghue et al., 2020a). For example, a change in a relative power measure could
421 arise from a change in band-specific power of interest, or be due to a change in aperiodic
422 component that changes the measured power across all frequencies that is used as the
423 denominator.

424 Explicitly measuring aperiodic activity requires methods that explicitly conceptualize both
425 aperiodic and periodic activity, to avoid erroneously attributing aperiodic activity as oscillatory
426 changes. Methods that define and measure oscillatory activity relative to aperiodic activity,
427 including previously introduced methods such as spectral parameterization (Donoghue et al.,
428 2020b) and eBOSC (Kosciessa et al., 2020), are designed to measure and control for aperiodic
429 activity, and so address this issue. There are also dedicated methods for measuring aperiodic

430 activity. For example, the irregular-resampling auto-spectral analysis (IRASA) method leverages
431 the scale-free nature of aperiodic activity by proposing a resampling procedure to isolate aperiodic
432 activity (Wen & Liu, 2016). IRASA can be used to separate and measure aperiodic neural activity,
433 after which analyses can evaluate each component to examine whether measures of interest
434 specifically reflect the intended component. Overall, controlling for aperiodic activity requires
435 employing an oscillation detection step and evaluating oscillatory power relative to the aperiodic
436 component in order to assess whether measured changes are capturing oscillatory or aperiodic
437 activity.

438



439

440 **Figure 3: Variations in aperiodic activity influence band-power measures. A)** Examples of aperiodic
 441 white (black) and pink (red) noise signals that display different patterns of power across frequencies, as
 442 seen in their power spectra. Shaded in blue is the canonical alpha range, with time-series filtered in the
 443 alpha-range shown in the inset. Note that the pink noise signal appears to have increased 'alpha' power.

444 **B)** Simulated combined signals containing both aperiodic and oscillatory power (black), and a transformed
 445 version of the signal with the same periodic component with a change in the aperiodic component (red),
 446 after being rotated in the spectral domain. Note that in A & B, what appears to be band-specific changes
 447 actually reflect differences in aperiodic activity.

448 **C)** A comparison between power spectra for combined signals simulated with the same oscillatory component with different aperiodic activity. Shading reflects
 449 different frequency bands, including delta (yellow), theta (green), alpha (blue), beta (purple) and gamma
 450 (red).

451 **D)** Absolute differences in power, calculated separately for each frequency band, for the spectra in
 452 C. Note that despite the difference in the data being simulated as a change in the aperiodic component, a
 453 band-by-band analysis suggests a pattern of changes across distinct frequency bands.

454 **E)** Relative alpha power (bottom) is calculated as absolute band power (top left), divided by the power across all frequencies
 455 (top right). Note that despite no difference in the amount of alpha power, there is measured change in
 456 relative power, due to systematically different aperiodic activity between the signals.

456

457 #4 Neural oscillations are variable across time

458 Why this matters

459 Neural oscillations often display burst-like temporal dynamics (Lundqvist et al., 2016;
460 Sherman et al., 2016) and are rarely, if ever, completely consistent and continuous. These
461 temporal dynamics of neural oscillations are a potentially important feature; for example, the rate
462 of burst events has been found to be predictive of behavior across tasks and species (Shin et al.,
463 2017), including in investigations of working memory (Lundqvist et al., 2016) and motor activity
464 (Wessel, 2020). Some generative models of oscillations predict non-continuous events in a way
465 that is consistent with what is seen in empirical data (Sherman et al., 2016).

466 Despite this, many methods implicitly assume stationarity of the signal under study, when
467 analyzing, for example, average band power across time or trials. In such cases, variability of
468 oscillation presence or temporal dynamics can be misinterpreted as differences in power. For
469 example, in simulations with stochastic onset and offset of oscillatory activity, signals can display
470 different proportions of the data with oscillatory activity present, with the oscillatory power when
471 present is equivalent (Fig. 4A). Measured power in such cases reports a different amount of band
472 specific power, typically interpreted as reflecting a change in the overall amplitude of the
473 oscillation, however, measured differences can be due to temporal variability (Fig. 4B). These
474 kinds of averaging effects are also important in scenarios such as time-frequency analyses that
475 average across trials, which may create an illusion of sustained activity in averaged data (Feingold
476 et al., 2015; Jones, 2016). This can happen if individual trials have burst-like temporal dynamics
477 that occur at different times across different trials, which can average together in a way as to
478 suggest a sustained response in average data, despite such continuity not occurring in any
479 individual trial (Fig. 4C). The temporal variability of neural oscillations motivates the importance
480 of considering single trial dynamics (Kosciessa et al., 2020; Rey et al., 2015; Stokes & Spaak,
481 2016).

482 Oscillatory bursts can vary in multiple ways that can lead to similar measured changes in
483 band power, which may be misinterpreted as reflecting changes in tonic band power. This
484 includes changes in burst duration (Fig. 4D), burst occurrence (Fig. 4E), or burst amplitude (4F),
485 each of which can vary within or between analyzed time periods (Quinn et al., 2019; Zich et al.,
486 2020). Understanding the different sources of variability has implications on how these signals
487 should be interpreted, as a change in the length, number, or size of bursts each likely reflect
488 different circuit mechanisms and putative relationships to neural function. However, this can not

489 be appropriately evaluated unless methods acknowledge oscillations as potentially transient, with
490 potential variability in rate, timing, and duration as well as amplitude (van Ede et al., 2018).

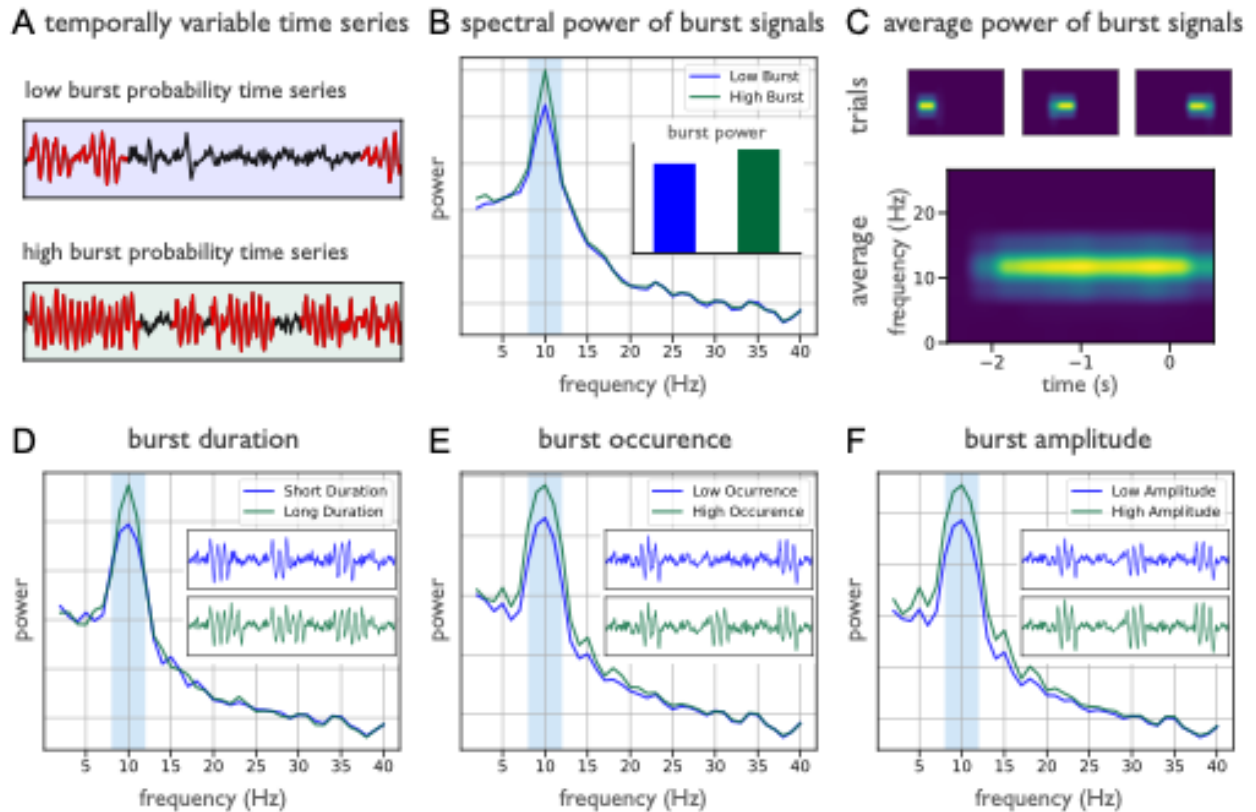
491 Recommendations

492 Analyses of neural oscillations must therefore evaluate whether temporal variability, rather
493 than overall power, may be driving measured changes. In order to address temporal variability,
494 both the spectral and temporal domain have to be considered together (Zich et al., 2020). Time-
495 frequency analyses, such as spectrograms, can be used to examine spectral properties across
496 time in order to adjudicate between changes in the average power of oscillations and changes in
497 their temporal dynamics. In doing so, it is important to analyze single-trials (Rey et al., 2015;
498 Stokes & Spaak, 2016), to avoid misinterpreting averaged power. If reporting spectrograms,
499 single-trial examples should be included in order to evaluate whether apparent sustained activity
500 is truly sustained, or arises as a result of averaging many short bursts.

501 Burst detection methods can also be applied to identify segments of the signal in which
502 oscillations are present, which can then be characterized in terms of the durations of the bursts,
503 the number of bursts, and/or the amplitude of the bursts. A common approach for burst detection
504 is to use an amplitude threshold, detecting segments of power in which frequency specific power
505 is greater than a chosen threshold level (Feingold et al., 2015). The previously described eBOSC
506 algorithm (Kosciessa et al., 2020) can be considered to be a threshold based burst detection, in
507 which the threshold is based on the aperiodic component, and can be used for burst detection.

508 Other algorithms for burst detection include matching pursuit, in which a dictionary of
509 atoms, which can include oscillatory bursts, is fit to the data, providing potentially more accurate
510 estimates of burst onset and duration (Chandran KS et al., 2018). Alternatively, methods such as
511 hidden markov modelling can be used, which seek to characterize state transitions, and can be
512 used to model transitions into and out of oscillatory states in a probabilistic way (Quinn et al.,
513 2019; Vidaurre et al., 2016). Time-domain measures that identify oscillations by characterizing
514 individual cycles, further described in #5, can also be used to detect and analyze the number and
515 duration of bursts, and their cycle-by-cycle properties (Cole & Voytek, 2019; Schaworonkow &
516 Nikulin, 2019). After detection, analyses of burst-like neural activity typically involve subsequent
517 analysis of the identified bursts, in order to evaluate whether they are changing in their duration,
518 occurrence, and/or amplitude.

519



520

521 **Figure 4: Temporal dynamics of neural oscillations influence spectral measures.** **A)** Two simulated
 522 signals with lower (top; blue) and higher (bottom; green) levels of bursting activity in the alpha band,
 523 simulated with probabilistic burst onset and offset. Segments identified as bursts are shaded in red. Note
 524 that oscillation power, when present, is the same in both signals. **B)** Power spectra for the signals in A.
 525 Note the difference in size of the alpha peak, suggesting a difference in alpha power between the signals.
 526 However, when quantifying the power within the bursts (inset bar plot), the power is found to be
 527 approximately the same. The apparent difference in power is due to differences in temporal variability. **C)**
 528 Temporal variability can lead to spurious sustained power in averaged results. Spectrograms for individual
 529 trials (top) show short bursts of oscillatory power, which average to create what appears to be a sustained
 530 response (bottom). **D-F)** Measured differences in power can arise due to multiple features of bursting
 531 oscillations, including changes in the duration (**D**), occurrence (**E**), and/or amplitude (**F**) of the bursts. In
 532 these simulations, one feature differed between the two time series, while all others were held constant.
 533 Each feature creates a similar difference in the resultant alpha peaks, demonstrating that measured power
 534 can reflect multiple facets of temporal variability of analyzed time series.

535

536 #5 Neural oscillations are non-sinusoidal

537 Why this matters

538 The waveform shape of neural oscillations is often non-sinusoidal (Cole & Voytek, 2017;
539 Jones, 2016), as seen, for example, in the arc-shaped sensorimotor mu-rhythm, visual alpha,
540 which can be triangular, and the sawtooth-shaped hippocampal theta-rhythm. These waveform
541 properties of neural oscillations may reflect physiological properties, for example the
542 synchronization of neural activity (Schaworonkow & Nikulin, 2019), spiking patterns of underlying
543 neurons (Cole & Voytek, 2018), or behavioral correlates such as running speed (Ghosh et al.,
544 2020). Waveform shape can therefore be an important feature of interest, with potential to impose
545 constraints on generative circuit models of oscillations (Sherman et al., 2016) as well as time
546 constants of involved synaptic currents.

547 The variable waveform shape of oscillations also creates substantial methodological and
548 interpretation hurdles, due to the assumed sinusoidal basis underlying most methods. For
549 instance, estimating instantaneous phase typically involves narrowband filtering the signal before
550 applying a Hilbert transform. Applying a narrowband filter on data with variations in waveform
551 shape can be problematic, as the phases of sinusoidal outputs of narrowband filtering will not
552 correspond to phases of a non-sinusoidal signal (Fig. 5A). This occurs because in the spectral
553 domain, nonsinusoidal shapes are represented by power across multiple frequencies, and if the
554 signal content in the harmonic frequencies is removed, the resulting filtered signal will have shifted
555 peaks and troughs compared to the original non-sinusoidal signal (Fig. 5A). This is an important
556 consideration for any analyses that examine cycle properties, such as the location of signal peaks
557 and troughs, as putatively corresponding to specific physiological states. For analyses that rely
558 on exact temporal characteristics (e.g. investigating the effects of pre-stimulus phase on
559 behavioral measures), controlling for waveform shape may be beneficial.

560 In spectral analysis, non-sinusoidal waveforms are reflected in the power spectrum as
561 harmonics occurring at multiples of the dominant frequency, as illustrated in Fig. 5B. This can
562 result in interpreting these separate peaks as independent physiological rhythms. In the case of
563 an arc-shaped mu-rhythm, for example, the waveform shape of the oscillation will create peaks
564 in both the alpha- and beta-frequency ranges. This may be interpreted as separate alpha- and
565 beta-rhythms with an assumed phase- and amplitude-coupled relationship, when in reality only
566 one non-sinusoidal rhythm is present. Differentiating between those situations is complicated by
567 the fact that several types of rhythms can be found across the cortex (see section #6). Fig. 5C

568 shows how the degree of non-sinusoidality is reflected in the power of harmonic frequencies, with
569 higher power in the harmonic frequency range for increasing non-sinusoidality. This should be
570 considered when evaluating differences in spectral power between conditions, to control for
571 potential changes in waveform shape.

572 The spurious coupling that waveform shape can induce between frequencies (Kramer et
573 al., 2008) is especially important when considering measures such as phase-amplitude coupling
574 that are greatly influenced by waveform shape (Cole et al., 2017; Lozano-Soldevilla et al., 2016).
575 Waveform shape can result in systematic changes in the amplitude at harmonic frequencies, as
576 seen in Fig. 5D, which can depend on the phase of the base oscillation, as quantified in Fig. 5E.
577 This results in significant measures of cross-frequency phase-amplitude coupling. Numerically,
578 these values are not objectionable, as they reflect a relationship between frequencies in the
579 spectral domain. However, there is possible fallacy in the interpretation, if this relationship is taken
580 to reflect significant coupling between *independent* rhythms, when in fact no such interaction
581 between multiple rhythms need exist. Because of these methodological limitations, careful work
582 needs to be done to adjudicate between phase amplitude coupling measures that reflect
583 waveform shape versus those that truly reflect nested oscillations (Giehl et al., 2021; Vaz et al.,
584 2017).

585 Recommendations

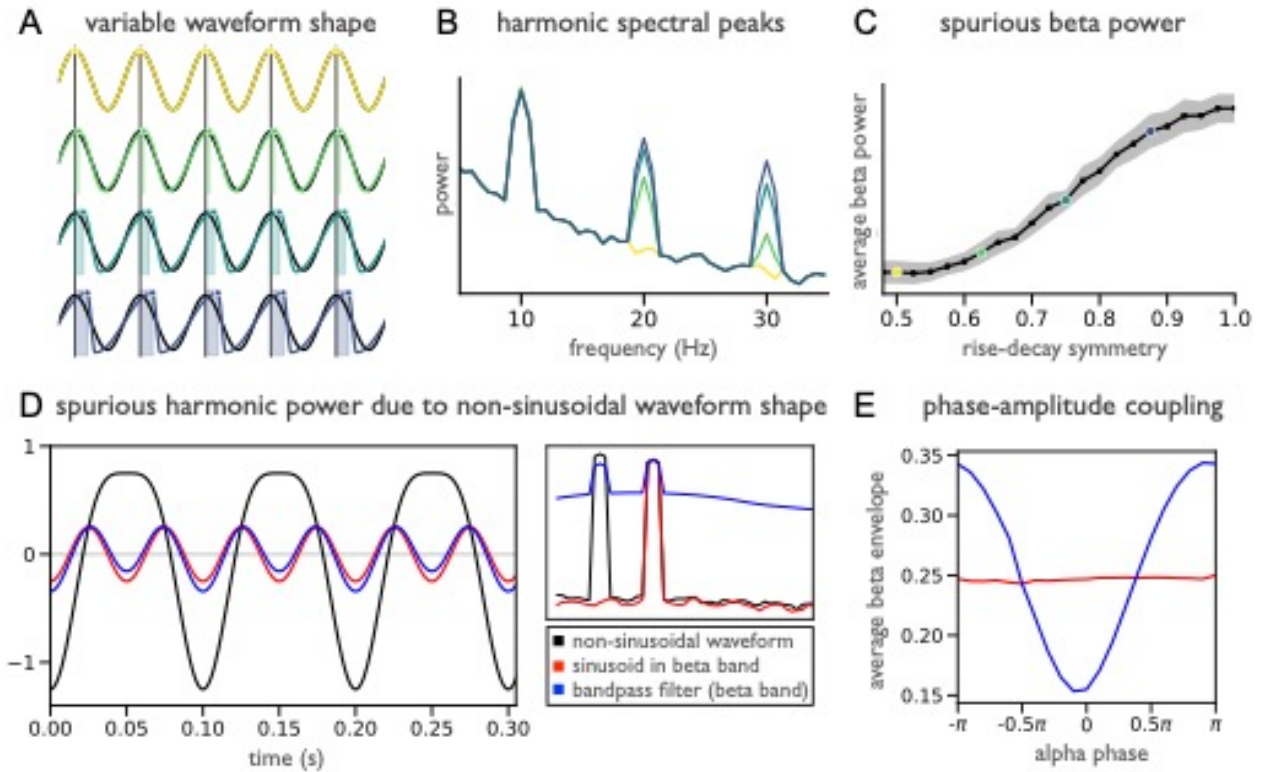
586 In order to evaluate and control for waveform shape, explicit measurement of waveform
587 and cycle properties should be done. Time domain measures of individual cycles can be used to
588 characterize waveform shape by, for example, calculating measures such as the rise/decay
589 symmetry or peak sharpness (Cole & Voytek, 2019; Schaworonkow & Nikulin, 2019). Other
590 methods aim at learning and grouping waveforms into observed categories, for example through
591 attempting to learn recurring patterns in the data by sliding-window matching (Gips et al., 2017)
592 or by attempting to learn a dictionary of observed shapes in the data and finding occurrences of
593 particular waveforms in the data based on templates (Barthélemy et al., 2013; Brockmeier &
594 Principe, 2016; Jas & Dupré, 2017).

595 In the frequency domain, specific waveforms can create stereotypical patterns in power
596 spectra and time-frequency representations, which can complicate the detection of oscillations
597 (see #1). If spectral peaks are present at exact multiples of slower frequencies, quantifying
598 waveform shape may help to distinguish between an independent oscillation at that particular
599 frequency or harmonic spectral peaks induced by waveform shape. Since different waveform
600 shapes may exhibit similar time-frequency representations (Jones, 2016), time-domain analyses

601 may be required to evaluate if and how waveform shape is contributing to spectral
602 representations.

603 For cross-frequency coupling analysis, the frequency extent of local coupling within a
604 region (e.g., for phase amplitude coupling, the range of higher frequencies that are coupled to the
605 low frequency phase) can suggest whether it is likely to be genuine oscillatory coupling or a shape
606 effect (Cole et al., 2017; Vaz et al., 2017), with narrow ranges at exactly multiples of the base
607 frequencies indicative of possible coupling caused by waveform shape. Applying and comparing
608 multiple measures of cross-frequency coupling can dissociate harmonic and non-harmonic
609 phase-amplitude coupling (Giehl et al., 2021). More generally, frequency domain methods such
610 as bicoherence, a measure of non-linear interactions between frequencies, can also be used to
611 investigate waveform shape in the frequency domain (Bartz et al., 2019).

612



613 **Figure 5: Waveform shape of neural oscillations influences power and coupling measures.** **A)** Four
 614 different time domain signals with varying rise-decay asymmetry (colored traces) and their narrowband
 615 filtered versions (black traces). Narrowband filtering of asymmetric oscillations shifts the peak times of the
 616 signals as indicated by the shaded regions marking the distance between the peaks of original signal and
 617 the filtered version. **B)** In the corresponding power spectrum, there are emerging spectral peaks at harmonic
 618 frequencies (exactly two and three times the frequency) as a result of the asymmetry. **C)** The scale of these
 619 harmonic peaks relates to the asymmetry, such that increasing waveform asymmetry can exhibit as
 620 increased power in the beta-frequency range. **D)** Non-sinusoidal rhythms can also create spurious phase
 621 amplitude coupling. A 10 Hz non-sinusoidal alpha signal is band-pass filtered around the beta peak
 622 frequency (15 - 25 Hz). The beta signal shows deviations in amplitude depending on alpha phase driven
 623 by the non-sinusoidal waveform shape (inset shows power spectra for each signal). **E)** Phase amplitude
 624 coupling is quantified by calculating beta envelope as a function of alpha phase. In contrast to a pure beta-
 625 sinusoid, the beta envelope from the non-sinusoidal signal shows a minimum for a specific alpha phase,
 626 indicating phase-amplitude coupling, which is driven by the waveform shape of the alpha rhythm.

627

628 #6 Multiple oscillations coexist across the brain

629 Why this matters

630 Non-invasive recordings of neural oscillations reflect aggregate activity across relatively
631 large cortical areas. Through volume conduction, a term used to describe the propagation of
632 electrical fields from their original source across tissues to recording sensors, recording
633 electrodes can reflect activity from multiple local sources, as well contributions from more distant
634 sources that overlap both spatially as well as temporally (Buzsáki et al., 2012; Nunez &
635 Srinivasan, 2006). For instance, in the context of MEG/EEG, there are several alpha-rhythm
636 sources, with locations in somatosensory, occipital, parietal and temporal cortex (Hindriks et al.,
637 2017), which can be co-active at the same time. In many studies, recordings are analyzed in
638 sensor space, by directly analyzing activity from recording electrodes. In such cases, the
639 aggregate signal may appear markedly different from the underlying sources of interest due to
640 the spatial and temporal overlap of multiple distinct sources. Measures applied to these combined
641 signals may therefore not accurately reflect the underlying sources, with distortions in measures
642 of temporal dynamics or waveform shape (Schaworonkow & Nikulin, 2019).

643 Examining how spectral and time domain measures can be affected by overlapping
644 sources is shown in an example in which sensor space activity from a single electrode is
645 composed of activity from two underlying sources in the parietal and visual cortices (Fig. 6A). In
646 the spectral domain, this configuration can result in two peaks in the alpha-frequency range (Fig.
647 6B), when the two sources have slightly different peak frequencies. This has been observed in
648 empirical data as ‘double alpha’ or ‘split alpha’ peaks (Chiang et al., 2008). Analyses in sensor
649 space may lead to the interpretation that a specific circuit generates signals with two
650 simultaneously present peak frequencies, which in turn will influence theories of generating
651 mechanisms. Spatial summation of multiple underlying rhythms of similar peak frequencies can
652 also mask temporal features of interest of the underlying rhythms, as seen in Fig. 6C, due to
653 constructive and destructive interference effects (Schaworonkow & Nikulin, 2019). Phase
654 differences between sources of similar frequencies can attenuate the oscillation in sensor space,
655 due to interference, even though oscillatory power has not changed in the underlying sources.
656 This may lead to erroneous interpretations regarding changing oscillatory power of the sources,
657 when it may be that only their relative temporal relationship has changed.

658 Inter-regional connectivity measures are also impacted by the simultaneous presence of
659 multiple sources. Computing connectivity measures using sensor space signals can lead to

660 spurious findings, because volume conduction influences these measures (Haufe et al., 2013; J.
661 M. Palva et al., 2018; S. Palva & Palva, 2012; Schoffelen & Gross, 2009). Because individual
662 sources propagate to multiple sensors, regularities in amplitude and phase will be present across
663 multiple sensors. This can yield highly significant statistical relationships between electrodes,
664 reflecting signal content that is present due to a common source rather than genuine interregional
665 coupling, which may lead to erroneous interpretation of connectivity between oscillatory sources.

666 Recommendations

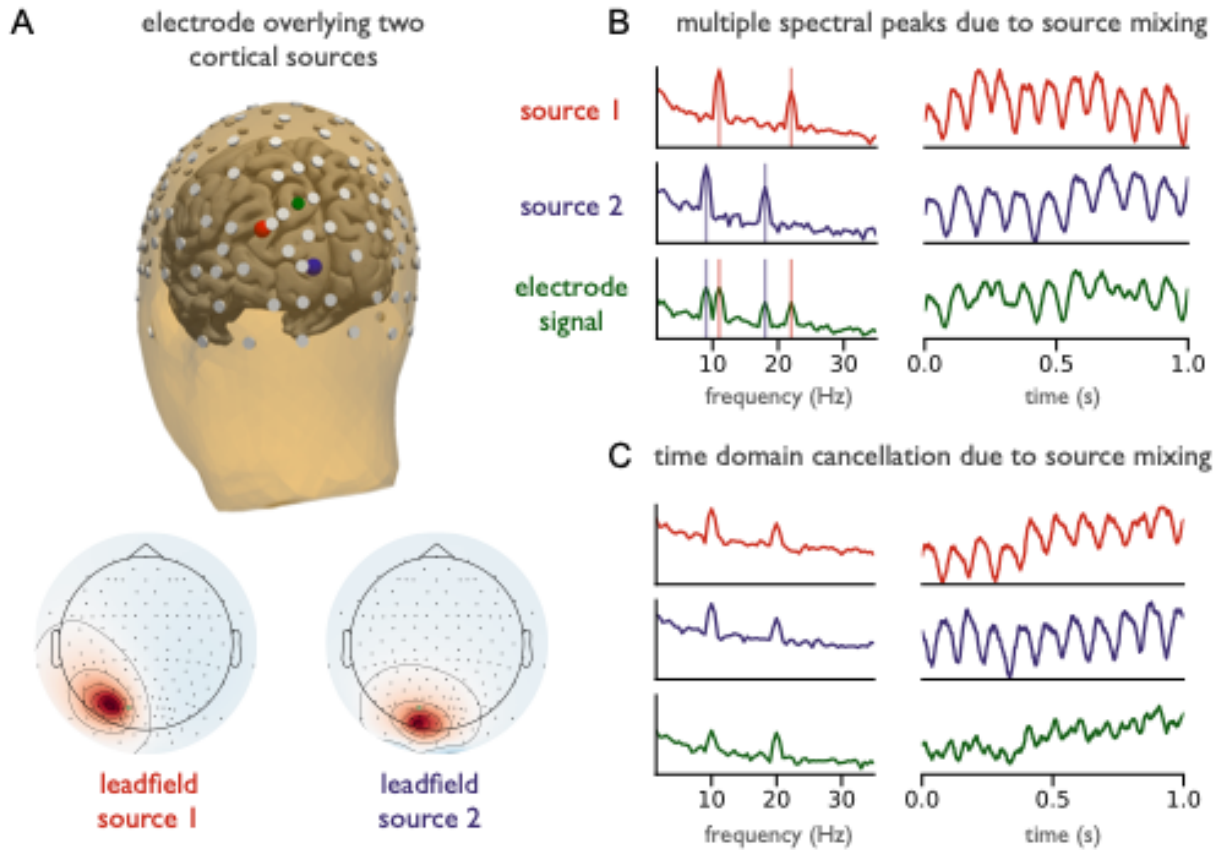
667 Due to overlapping sources, analyzing sensor level time series or power spectra can be
668 misleading regarding which aspects of the oscillation are present and/or are changing. Whenever
669 possible, sensor space analysis should be complemented by source-level analysis. Source
670 separation methods can be applied to attempt to separate different narrowband periodic
671 components in the signal, which can help to reveal features that are not visible in sensor space
672 data, as well as helping to localize sources. There are many possible approaches for source
673 separation. Because inferring the activity of many more sources than channels is not possible,
674 constraints are needed to arrive at a specific decomposition. The choice of the appropriate
675 method also depends on the specific goals of source separation, including, for example, localizing
676 activity to specific regions and/or decomposing time series into components based on statistical
677 properties.

678 Based on these goals, two main approaches with different optimization criteria can be
679 used for estimating source activity from sensor space activity. The first main type of methods use
680 anatomical information to constrain the inverse solution based on individual or template structural
681 MRI, in combination with methods such as beamformer or minimum norm estimation techniques
682 (Hauk et al., 2019). The second main type of methods are agnostic to anatomical information and
683 rely solely on the statistical structure of signals across channels. In this approach, channel activity
684 is assumed to be a linear mixture of multiple underlying sources, defined by a leadfield matrix,
685 which describes how individual sources map onto sensors (Parra et al., 2005). By assuming
686 specific statistical properties of the source time series as well as mixing properties, demixing can
687 be attempted. Methods in this realm include joint decorrelation (de Cheveigné & Parra, 2014) or
688 independent component analysis (Hyvärinen & Oja, 2000). In the context of investigating neural
689 oscillations, there are variants that specifically maximize SNR of narrowband oscillatory
690 components, while minimizing SNR in flanking bands or in comparison to broadband activity. For
691 enhancing oscillatory SNR, spatial-spectral decomposition (Nikulin et al., 2011) or generalized
692 eigendecomposition (Cohen, 2017b) can be used. The Common Spatial Patterns algorithm

693 (Koles, 1991) and its variants (Lotte & Cuntai Guan, 2011) can be used for maximizing differences
694 in narrowband activity between task conditions. For investigating relationships between
695 narrowband activity and a continuous variable, Source Power Correlation analysis (Dähne et al.,
696 2014) may be of interest. Spatial filtering methods can also be used as a preprocessing step for
697 dimensionality reduction (Haufe, Dähne, et al., 2014), easing statistical comparisons and
698 computational needs.

699 Components that result from source separation need validation, since different methods
700 or parameter settings can yield highly different results, and solutions are not guaranteed to reflect
701 physiologically meaningful activity. As such, source separation can be non-trivial and has its own
702 set of methodological considerations as well as reporting guidelines (Cohen & Gulbinaite, 2014;
703 Haufe, Meinecke, et al., 2014; Mahjoory et al., 2017). These guidelines can be used to evaluate
704 robustness of the solution, such as with goodness of fit and/or localization error metrics, and to
705 adequately convey reconstruction quality and method details to the reader.

706



707 **Figure 6: Multiple simultaneous rhythms can interfere and impact sensor level data.** **A)** A realistic
 708 head model with two oscillatory sources (red and blue) placed in the posterior cortex which project on the
 709 highlighted electrode (green). Underneath are the topographies of the two sources that contribute to the
 710 recording electrode. The leadfield coefficients for the two sources have approximately equal values,
 711 indicating equal contribution to the activity recorded at the green electrode. **B)** In this simulation, the
 712 electrode signal (green; bottom) reflects multiple underlying sources, including two distinct rhythmic
 713 components, with slightly different peak frequencies. These sources can be seen as two spectral peaks in
 714 the power spectrum. **C)** A separate simulation of two oscillatory sources with the same peak frequency,
 715 with a phase difference. Due to a phase difference of π , the two sources sum together destructively. In this
 716 scenario, interference of the sources cancel each other out at the electrode level, even though the
 717 oscillatory power of the individual sources is stable and consistent.

718 #7 Measures of neural oscillations require sufficient signal-to-noise ratio

719 Why this matters

720 Neural oscillations are embedded in complex recordings containing multiple rhythmic
721 signals, aperiodic activity, and transient events. Analyzing oscillatory signals of interest requires
722 defining features of interest (signal), and extracting this signal from the rest of the data (noise).
723 As with all measures, methods for analyzing oscillations require an adequate signal to noise ratio
724 (SNR). Indeed, ubiquitous processing steps such as filtering are used largely in order to increase
725 the SNR (Widmann et al., 2015). Many of the considerations thus far (detecting oscillations,
726 adjusting frequency ranges, controlling for aperiodic activity, burst detection, and source
727 separation) can all be conceptualized as aiming to increase SNR by tuning analyses to specific
728 properties of the data. Beyond these specific properties, applied measures can still be
729 inaccurately estimated if SNR is low or variable.

730 The SNR of oscillatory activity relates to the ratio of oscillatory power to noise, typically
731 the aperiodic background. Oscillatory power is a dynamic property, which can be seen by the
732 variable height of oscillatory peaks over and above the aperiodic component (Fig. 7A). Many
733 experimental paradigms will change oscillatory power, as presentation of stimuli may result in
734 event-related attenuation of oscillations (Pfurtscheller & Lopes da Silva, 1999). This change in
735 oscillatory power changes SNR, which in turn may influence accuracy and stability of other
736 oscillatory measures such as instantaneous phase and frequency. When SNR is high, estimations
737 of phase and frequency can be reliably estimated (Fig. 7B). However, when SNR is low,
738 estimation can be very noisy (Sameni & Seraj, 2017) as can be seen in Fig. 7C, leading to
739 artifactual large variations, often referred to as phase slips.

740 Changes in oscillatory power which change SNR and corrupt phase estimations can lead
741 to inaccurate estimates of derived measures, such as the phase-locking value
742 (Muthukumaraswamy & Singh, 2011) or inter-trial coherence (van Diepen & Mazaheri, 2018). Low
743 SNR makes it difficult to reliably extract oscillations of interest (Fig. 7D), leading to variable phase
744 estimates (Fig. 7E). When computing coupling measures on such estimates, differences in SNR,
745 absent any true changes in phase alignment, can erode the detection of phase-locking between
746 two signals (Fig. 7F). Unstable estimation of oscillatory measures can also propagate to
747 multivariate analysis, such as cross-frequency coupling, whereby oscillatory power changes that
748 influence SNR can lead to a change in measured cross-frequency coupling (Aru et al., 2015).

749 Time domain analyses, such as those designed for analyzing waveform shape, are also strongly
750 dependent on their being adequate SNR to meaningfully measure the properties of interest.

751 In cases of low SNR, unreliable estimates could, for example, lead to false-negatives due
752 to noisy estimations that are not able to adequately capture measures of interest. Conversely,
753 certain analyses may return false positive results, if the measured variability of the signal is mis-
754 interpreted as a feature of interest, and/or leads to an artifactual measured change between
755 conditions due to variable SNR. This may be an issue when comparing between groups who are
756 known to have differences in relative power of oscillations, and/or when comparing within
757 participants across conditions that may have different SNR.

758 Recommendations

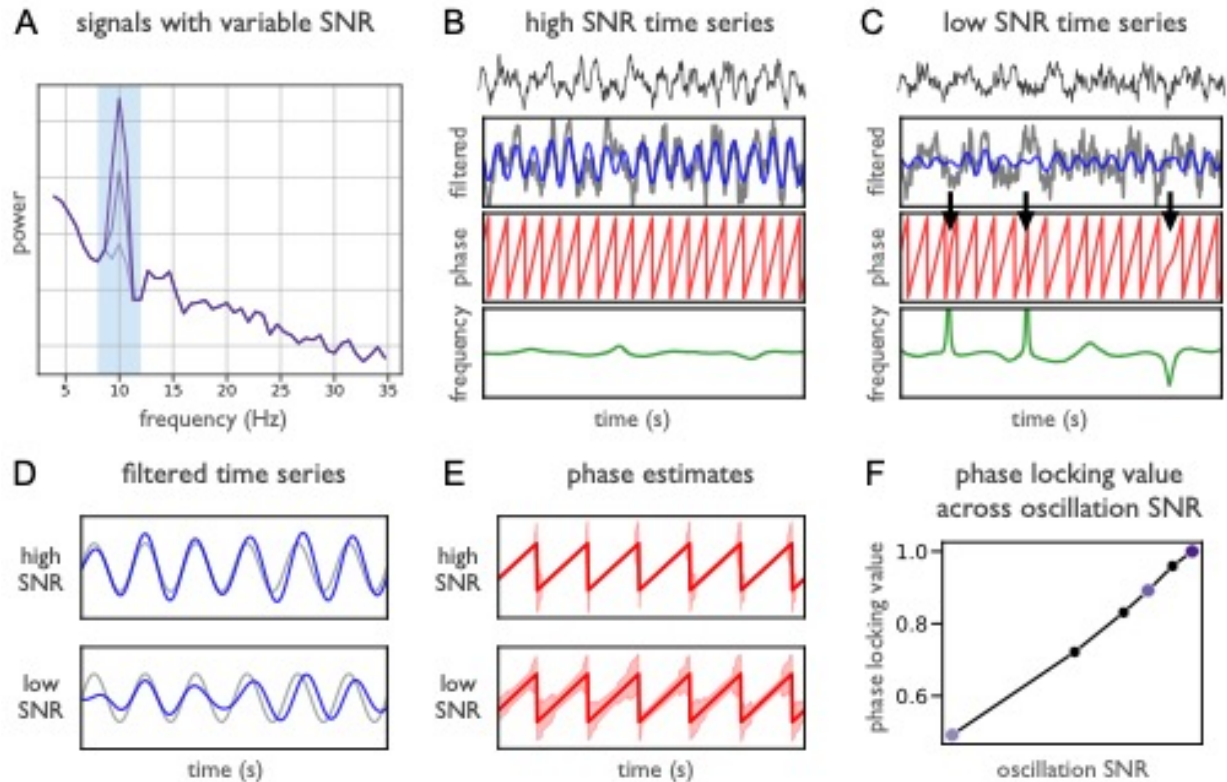
759 Considering the SNR required for stable estimation of measures of oscillations starts by
760 choosing appropriate experimental designs. When designing the protocol and tasks,
761 experimenters should consider what is known about the reliability and effect size of effects of
762 interest, and consider doing a power analysis to design well powered studies. This includes
763 considering recording modalities, as different modalities have different sensitivities to different
764 source locations (Piastra et al., 2020), as well as the different temporal, spatial, and frequency
765 resolutions they offer. When recording the data, best practices should be employed to minimize
766 non-neuronal noise, and use appropriate preprocessing in order to increase the quality of the data
767 with the respect to desired analyses (Keil et al., 2014; Pernet et al., 2020).

768 Once recordings have been collected, or if considering existing datasets for potential re-
769 analysis, signal-to-noise ratio has to be considered to validate if the dataset is appropriate for the
770 desired analyses. This requires explicitly measuring SNR to verify that applied measures are
771 robust in the SNR regime of the data. If the SNR is too low to provide accurate measurements,
772 the analyses may be non-viable, as any measurements will be uninterpretable. If the analysis can
773 be run, then SNR should still be continuously verified, to evaluate whether potential changes of
774 SNR across time or between conditions may explain measured changes in results (van Diepen &
775 Mazaheri, 2018).

776 General approaches for optimizing SNR include good filter design (de Cheveigné &
777 Nelken, 2019; Widmann et al., 2015), and using information about spectral estimators and signals
778 of interest to select the most appropriate methods to improve the accuracy and stability of
779 estimates (Chavez et al., 2006; Lepage et al., 2013). There are also specific methods for more
780 robust estimations of phase in low power situations, including Monte Carlo estimation (Sameni &
781 Seraj, 2017) and applying a Kalman smoother (Mortezapouraghdam et al., 2018). Many of the

782 previously described methods such as detecting oscillatory peaks, using individualized frequency
783 ranges, and using burst detection can all improve SNR. Source separation techniques, including
784 those that explicitly optimize SNR (Cheveigné & Arzounian, 2015; Nikulin et al., 2011) can be
785 used to extract oscillatory components with higher SNR.

786



787 **Figure 7: Low oscillatory signal-to-noise ratio impacts measures.** **A)** Power spectra for simulated
 788 signals with variable SNR for an alpha oscillation, as seen in the different peak heights. **B)** One of the
 789 simulated signals, with a high SNR, with the alpha filtered signal (top; blue), from which the instantaneous
 790 phase (middle; red) and frequency (bottom; green) are computed. Note that the simulated signal has
 791 consistent phase and frequency. **C)** The same as B, for a signal with low SNR. Note that in this case, the
 792 estimates of phase and frequency are variable, due to misestimations because of the low SNR. This leads
 793 to phase slips, indicated by the arrows, in instantaneous phase, which also leads to erratic estimates of
 794 instantaneous frequency. **D)** Filtered versions of high and low SNR signals. In the simulated signals, the
 795 underlying signals (grey) are the same, other than a power difference, and have uniform phase. The filtered
 796 traces (blue) diverge from the underlying signal, especially in the low SNR signal. **E)** Phase estimates of
 797 the signals in D, in which the solid red is the true phase of the simulated oscillation, and the shading reflects
 798 the standard deviation of estimated phase across multiple iterations of phase estimation within each SNR
 799 regime. This shows that there is higher variance of phase estimates with lower SNR. These unstable phase
 800 estimates will impact subsequent measures, such as phase coupling. **F)** The phase locking value computed
 801 between a high powered oscillation, and simulated signals with decreasing power, as shown in A. Note that
 802 the simulated oscillations all have the same simulated phase time course, such that there is an expected
 803 phase locking value of 1, and any estimates below this are misestimations due to low power.

804 Discussion

805 How, and to what extent, neural oscillations are mechanistically involved in cognition
806 remains undetermined. This lack of clarity likely arises in part from imprecisions in our
807 methodological approaches for analyzing oscillations that, in turn, give rise to inconsistent results.
808 Here, we highlight specific methodological considerations for analyzing and interpreting neural
809 oscillations, providing explicit recommendations regarding each topic. These considerations
810 acknowledge the heterogeneity of neural oscillations and embrace this complexity as an
811 opportunity to consider ideas and interpretations that may help us to further understand our data.
812 Oscillations vary in their presence and frequency, co-exist with dynamic aperiodic activity, have
813 idiosyncratic temporal and waveform shape properties, overlap with one another, and require
814 sufficient SNR to appropriately analyze. These topics also demonstrate that there is an increasing
815 set of features that can be defined for neural oscillations, with an increasing toolkit of estimation
816 methods. Hopefully, these recommendations can serve as guidelines for potentially reducing
817 misinterpretations and conflicting results, and can increase clarity in our understanding of neural
818 oscillations.

819 These considerations relate broadly to studies investigating neural oscillations, including
820 investigations of endogenous activity, and/or of rhythmic neural activity that may be induced by
821 stimulus presentation (Doelling et al., 2019; Lakatos et al., 2008). The potential impact of the
822 considerations may vary across different studies. In many cases, these considerations may not
823 change the analyses or interpretations, but may still offer potential avenues for further analyses,
824 and deeper understanding of the data. In some situations, these considerations may greatly
825 impact results and interpretations, potentially reflecting fundamental confounds that do need to
826 be addressed, or even reflect issues that cannot be addressed by current methods, such that it
827 precludes particular analyses from being appropriately applied. Overall, with a range of possible
828 impacts, the general recommendation is to check for all of these possible issues, to identify which
829 topics may matter in each scenario, and proceed accordingly.

830 Though we present the considerations as seven distinct points, it is important to note that
831 these considerations do not manifest in isolation from one another and can interact. For example,
832 variable aperiodic activity (#3) can interfere with spectral peak (#1) and/or burst (#4) detection,
833 as it complicates approaches that use a threshold criterion to define bursts or spectral peaks.
834 Oscillations may also be difficult to detect (#1) and/or to individualize frequencies for (#2) if they
835 are temporally rare (#4), and/or have low SNR (#7). Further, waveform shape (#5) may
836 systematically vary in relation to underlying sources (#6) (Schaworonkow & Nikulin, 2019) and/or

837 detected peaks (#1) may be volume conducted from remote sources (#6), resulting, for example,
838 in ‘double alpha’ peaks due to the overlap of occipital and sensorimotor rhythms in the alpha-
839 band (Chiang et al., 2008). Multiple oscillatory features, such as power, waveform shape, burst
840 rate, etc., can covary. These potential multicollinearities need to be explicitly considered and
841 tested by robust analyses that control for multiple potentially confounding features by, for
842 example, addressing overlapping periodic and aperiodic activity (Donoghue et al., 2020b;
843 Kosciessa et al., 2020), controlling for waveform shape, which may result in spurious power-
844 and/or phase-coupling (Cole & Voytek, 2019; Schaworonkow & Nikulin, 2019), and examining
845 trial-by-trial dynamics that may be masked or conflated in average measures (Jones, 2016;
846 Stokes & Spaak, 2016; Zich et al., 2020).

847 This investigation used a simulation approach that attempts to mimic the properties seen
848 in empirical data, including dynamic aperiodic activity, and oscillatory components that can vary
849 across multiple features (Cole et al., 2019). Because ground-truth properties of physiological data
850 are not known in a way that can be used to evaluate the accuracy of applied measures, simulated
851 data are an important tool for diagnosing available methods. In using simulated data, we must
852 endeavor to reflect on our empirical data—simulating heterogeneous oscillatory features
853 embedded within dynamic aperiodic activity—in order to be representative of empirical data and
854 realistic use cases. As well as the tool used here, there are other approaches for simulating data,
855 including for specific modalities such as EEG (Krol et al., 2018), or that emulate neural circuits
856 (Neymotin, Daniels, et al., 2020), or whole brain recordings (Sanz Leon et al., 2013). Simulation
857 analyses should be employed when developing new analysis approaches, as novel methods
858 require validation and comparison to existing methods, such that best practice guidelines can be
859 continuously developed and updated. All time-frequency methods include settings that should
860 also be validated and explored. Sensitivity analyses, in which one repeats the analyses across
861 mild perturbations of method settings to evaluate the robustness of the measured results, should
862 be used to ensure that results are not overly dependent on specific parameter regimes.

863 Estimates of oscillatory features of interest are typically further analyzed and compared
864 using statistical methods. Notably, many neuroscientific parameters exhibit skewed distributions
865 (Buzsáki & Mizuseki, 2014), including oscillatory power (Kiebel et al., 2005). Therefore,
866 distributional properties of data should be carefully considered such that appropriate statistical
867 tests can be chosen (Maris, 2012; Maris & Oostenveld, 2007). This is especially important when
868 considering that power-law distributed variables can result in spurious correlations when using
869 methods that assume normality (Schaworonkow et al., 2015). Statistical analyses, in particular in
870 the context of new methods and measures, should also evaluate consistency across participants

871 (Grice et al., 2020), reliability within participants, and effect size measures, which can be
872 computed using estimation statistics (Calin-Jageman & Cumming, 2019). Considering effect sizes
873 can also aid in designing studies that are sufficiently powered (Button et al., 2013). Adopting the
874 best practices proposed here may also help to increase statistical power, insofar as they help to
875 better and more specifically characterize features of interest, improving SNR.

876 In our examples, we focused primarily on univariate measures, such as estimating
877 oscillatory power or phase. Issues that affect these estimates also propagate to derived
878 measures, such as correlations between amplitude or phase, as is done in functional connectivity
879 (Haufe et al., 2013) and cross-frequency coupling analyses (Aru et al., 2015). If phase estimates
880 are unreliable due to low oscillatory SNR (Sameni & Seraj, 2017), or if amplitude estimates are
881 biased by changes in aperiodic activity (Donoghue et al., 2020b), or if burst properties vary
882 between analyzed signals (Jones, 2016), then derived measures may fail to reflect the intended
883 oscillatory properties. Methodological limitations are likely to propagate and compound in
884 multivariate or mass univariate analyses, and must therefore be considered for any analyses
885 including, or built on top, of the univariate methods demonstrated here.

886 Though beyond the scope of this article, investigations of neural oscillations also require
887 employing best-practices for designing, collecting, and preprocessing data in order to ensure
888 sound research design, high quality data, and methodological validity. These considerations are
889 covered in available textbooks (Cohen, 2014; Hari & Puce, 2017), as well as individual reports
890 that discuss topics such as including best practices for reporting and conducting MEG/EEG
891 research (Gross et al., 2013; Keil et al., 2014; Pernet et al., 2020), pre-processing (de Cheveigné
892 & Arzounian, 2018), artifact rejection and data cleaning (Jas et al., 2017; Urigüen & Garcia-
893 Zapirain, 2015), and guides to using common software tools such as MNE (Gramfort, 2013; Jas
894 et al., 2018) and FieldTrip (Oostenveld et al., 2011; Popov et al., 2018). Other work also features
895 dedicated discussion for specific methods such as filtering (de Cheveigné & Nelken, 2019;
896 Widmann et al., 2015), phase estimations (Chavez et al., 2006; Lepage et al., 2013), functional
897 connectivity (O'Neill et al., 2018), and cross-frequency coupling analyses (Aru et al., 2015).

898 Broader strategies are also required for addressing reproducibility in the field of neural
899 oscillations, including pursuing replication studies, providing clear descriptions of methods and
900 results, and publishing null results (Cohen, 2017a). Open-science practices, including making
901 data and analysis code available, can help foster reproducibility and develop transparency
902 (Gleeson et al., 2017; Kathawalla et al., 2020; Voytek, 2016). Due to their computational nature,
903 investigations of neural oscillations also benefit from good code practice (Wilson et al., 2017).
904 Standardized procedures for organizing datasets also increase shareability, organization, and can

905 assist in standardized pipelines, making it easier to apply novel methods (Holdgraf et al., 2019;
906 Niso et al., 2018; Pernet et al., 2019). Adopting open science practices provides opportunities for
907 using open tools and datasets that can foster transparency and efficiently allow for revisiting the
908 evidence for how neural oscillations relate to cognition and disease.

909 Importantly, these considerations also reflect opportunities for developing new theory and
910 understanding of neural field data, which is still in many ways a mystery (Cohen, 2017c). Aperiodic
911 activity is itself a physiologically informative feature (Gao et al., 2017, 2020), reflecting processes
912 distinct from neural oscillations (Donoghue et al., 2020b; B. J. He, 2014). New methods provide
913 new opportunities, for example, the ability to jointly analyze multiple components of the data, such
914 as how oscillations and aperiodic activity jointly contribute to cognitive processing (Cross et al.,
915 2020). New features of interest offer the potential for better understanding underlying physiology
916 and putative computational roles of neural oscillations. For example, modelling that explicitly
917 considers waveform shape and/or burst properties has contributed to physiological models of
918 neocortical beta generation (Sherman et al., 2016), and models proposing mechanisms of beta
919 and gamma activity in working memory (E. K. Miller et al., 2018).

920 Our emerging understanding of the data under study and how to measure it provides new
921 vistas of opportunity for continuing to understand neural field data, and how it relates to cognition
922 and disease. These methods and topics reflect the current status of methodological
923 considerations for research related to neural oscillations. As our understanding of the many
924 complexities of neural data continues to evolve, future investigations of neural oscillations must
925 continue a consistent process of interrogating the assumptions of our methods and how they
926 relate to current knowledge of the data to validate measures of the data, and develop evolving
927 best practices.

928

929 **Conclusion**

930 Productively investigating neural oscillations requires dedicated and carefully applied
931 methods that reflect our current understanding of the data. As methodological validity is a
932 prerequisite for appropriate interpretation, analysis methods must reflect that neural field data
933 consists of a complex combination of multiple oscillatory components, variable aperiodic activity,
934 and transient events, within which oscillations vary across multiple dimensions. Here, we have
935 proposed a checklist of methodological considerations for neural oscillations, with
936 recommendations to 1) validate that oscillations are present; 2) verify that used frequency ranges
937 are appropriate; 3) control for potential confounds due to aperiodic activity; consider the 4)
938 temporal variation and 5) waveform shape of neural oscillations; 6) apply source separation, as
939 needed, to separate multiple oscillatory processes; and 7) evaluate that the SNR is adequate for
940 the analyses at hand. These considerations, and new methods that have been developed to
941 address them, reflect our emerging understanding of neural field data and offer new possibilities
942 for investigating, and ultimately, understanding, neural oscillations.

943

944 Materials and Methods

945 A simulation-based approach was used to create the demonstrations in this manuscript.
946 Simulated time series were created with the NeuroDSP toolbox (Cole et al., 2019), version 2.2.0.
947 In most cases, the time series were created as a combination of oscillatory and aperiodic activity,
948 sampled at 1000 Hz. Oscillatory activity was simulated as sine waves unless otherwise noted.
949 Each oscillation was simulated at a specific frequency, typically in the alpha band, unless
950 otherwise specified. Aperiodic activity was simulated by spectrally rotating white noise to the
951 desired $1/f$ exponent (Timmer & Konig, 1995). Aperiodic and oscillatory signal components were
952 weighted according to a specified variance and combined together in an additive manner. Across
953 all analyses, power spectra were estimated using Welch's method (Welch, 1967), using Hanning
954 windowed 1 second segments with 12.5% overlap. Filtering was done with finite impulse response
955 bandpass filters, with linear phase and filter lengths set to a default of 3 cycles of the highpass
956 frequency, and enforced to be odd (Type I). Canonical band ranges were defined as delta (2-4
957 Hz), theta (4-8 Hz), alpha (8-13 Hz), and beta (13-30 Hz), unless otherwise specified. Analysis
958 methods were also used as available in the NeuroDSP toolbox, or with custom code included in
959 the project repository (<https://github.com/voytekresearch/oscillationmethods>).

960 Several of the figure demonstrations used additional processing. For the peak detection
961 in Figure 1, the spectral peak was detected and quantified using spectral parameterization, which
962 models the power spectrum as a combination of aperiodic and oscillatory components, and can
963 be used to detect peaks of putative oscillatory power over and above the measured aperiodic
964 component (Donoghue et al., 2020b). For the individual frequency example in Figure 2, canonical
965 alpha was defined as ± 2 Hz around 10 Hz, and individualized alpha bands were defined as \pm
966 2 Hz around the individual peak frequency. For the demonstrations of varying aperiodic activity in
967 Figure 3, generated time series were spectrally rotated, in the same manner as done to simulate
968 the aperiodic activity (Timmer & Konig, 1995). Relative power was computed as the sum of power
969 in a frequency band of interest, divided by the sum of power across all frequencies in the
970 frequency range of 2-50 Hz.

971 For the temporal variation demonstrations in Figure 4, bursty oscillations were simulated
972 by specifying time segments that should include an oscillation, optionally controlling the duration,
973 occurrence, and amplitude of the bursts. Burst specific power was calculated by sub-selecting
974 segments of the data with an oscillation present. For the examinations of waveform shape in
975 Figure 5, oscillations were simulated as asymmetric sine waves, and the bicycle toolbox (version
976 1.0.0) was used to quantify waveform shape in the time domain (Cole & Voytek, 2019). For this,

977 signals were band-pass filtered around the frequency of interest (here: 10 Hz) to extract the time
978 points of zero-crossings of the signal. The time points were used to segment the broadband data
979 into cycles, determining several cycle parameters. For this example, simulated time series were
980 created with varying rise-decay symmetry, which is the ratio of time in the rising and decaying
981 segments of the oscillation, which creates asymmetric oscillations.

982 For the spatial mixing demonstration in Figure 6, the New York Head (ICBM-NY) was used
983 (Huang et al., 2016) as a head model. Two sources are placed in the posterior cortex, and the
984 corresponding sensor signals are calculated using the leadfield. Oscillations were simulated as
985 asymmetric waves, created as the sum of two sines waves with a fixed phase lag. Topographies
986 were visualized using MNE-python (Gramfort, 2013). In Figure 7, instantaneous measures were
987 computed by applying the Hilbert transform to signals that had been bandpass filtered into the
988 alpha range (8-12 Hz), taking the angle as the phase estimate, and using the derivative of the
989 instantaneous phase as a measure of instantaneous frequency. Phase synchrony was measured
990 using the phase locking value (Lachaux et al., 1999).
991

992 References

- 993
- 994 Aru, J., Aru, J., Priesemann, V., Wibral, M., Lana, L., Pipa, G., Singer, W., & Vicente, R. (2015).
 995 Untangling cross-frequency coupling in neuroscience. *Current Opinion in Neurobiology*,
 996 *31*, 51–61. <https://doi.org/10.1016/j.conb.2014.08.002>
- 997 Babiloni, C., Barry, R. J., Başar, E., Blinowska, K. J., Cichocki, A., Drinkenburg, W. H. I. M.,
 998 Klimesch, W., Knight, R. T., Lopes da Silva, F., Nunez, P., Oostenveld, R., Jeong, J.,
 999 Pascual-Marqui, R., Valdes-Sosa, P., & Hallett, M. (2020). International Federation of
 1000 Clinical Neurophysiology (IFCN) – EEG research workgroup: Recommendations on
 1001 frequency and topographic analysis of resting state EEG rhythms. Part 1: Applications in
 1002 clinical research studies. *Clinical Neurophysiology*, *131*(1), 285–307.
 1003 <https://doi.org/10.1016/j.clinph.2019.06.234>
- 1004 Barthélemy, Q., Gouy-Pailler, C., Isaac, Y., Souloumiac, A., Larue, A., & Mars, J. I. (2013).
 1005 Multivariate temporal dictionary learning for EEG. *Journal of Neuroscience Methods*,
 1006 *215*(1), 19–28. <https://doi.org/10.1016/j.jneumeth.2013.02.001>
- 1007 Bartz, S., Avarvand, F. S., Leicht, G., & Nolte, G. (2019). Analyzing the waveshape of brain
 1008 oscillations with bicoherence. *NeuroImage*, *188*, 145–160.
 1009 <https://doi.org/10.1016/j.neuroimage.2018.11.045>
- 1010 Başar, E. (2013). Brain oscillations in neuropsychiatric disease. *Dialogues in Clinical*
 1011 *Neuroscience*, *15*(3), 291–300. <https://doi.org/10.31887/DCNS.2013.15.3/ebasar>
- 1012 Başar, E., Başar-Eroğlu, C., Karakaş, S., & Schürmann, M. (2001). Gamma, alpha, delta, and
 1013 theta oscillations govern cognitive processes. *International Journal of Psychophysiology*,
 1014 *39*(2), 241–248. [https://doi.org/10.1016/S0167-8760\(00\)00145-8](https://doi.org/10.1016/S0167-8760(00)00145-8)
- 1015 Benwell, C. S. Y., London, R. E., Tagliabue, C. F., Veniero, D., Gross, J., Keitel, C., & Thut, G.
 1016 (2019). Frequency and power of human alpha oscillations drift systematically with time-
 1017 on-task. *NeuroImage*, *192*, 101–114. <https://doi.org/10.1016/j.neuroimage.2019.02.067>
- 1018 Brazier, M. A. B. (1958). The Development of Concepts Relating to the Electrical Activity of the
 1019 Brain. *The Journal of Nervous and Mental Disease*, *126*(4), 303–321.
- 1020 Brockmeier, A. J., & Principe, J. C. (2016). Learning Recurrent Waveforms Within EEGs. *IEEE*
 1021 *Transactions on Biomedical Engineering*, *63*(1), 43–54.
 1022 <https://doi.org/10.1109/TBME.2015.2499241>
- 1023 Bruns, A. (2004). Fourier-, Hilbert- and wavelet-based signal analysis: Are they really different
 1024 approaches? *Journal of Neuroscience Methods*, *137*(2), 321–332.
 1025 <https://doi.org/10.1016/j.jneumeth.2004.03.002>
- 1026 Bullock, T. H., McClune, M. C., & Enright, J. T. (2003). Are the electroencephalograms mainly
 1027 rhythmic? Assessment of periodicity in wide-band time series. *Neuroscience*, *121*(1),
 1028 233–252. [https://doi.org/10.1016/S0306-4522\(03\)00208-2](https://doi.org/10.1016/S0306-4522(03)00208-2)
- 1029 Button, K. S., Ioannidis, J. P. A., Mokrysz, C., Nosek, B. A., Flint, J., Robinson, E. S. J., &
 1030 Munafò, M. R. (2013). Power failure: Why small sample size undermines the reliability of
 1031 neuroscience. *Nature Reviews Neuroscience*, *14*(5), 365–376.
 1032 <https://doi.org/10.1038/nrn3475>
- 1033 Buzsáki, G., Anastassiou, C. A., & Koch, C. (2012). The origin of extracellular fields and
 1034 currents—EEG, ECoG, LFP and spikes. *Nature Reviews Neuroscience*, *13*(6), 407–420.
 1035 <https://doi.org/10.1038/nrn3241>

- 1036 Buzsáki, G., & Draguhn, A. (2004). Neural oscillations in cortical networks. *Science*, *304*(5679),
 1037 1926–1929. <https://doi.org/10.1126/science.1099745>
- 1038 Buzsáki, G., Logothetis, N., & Singer, W. (2013). Scaling Brain Size, Keeping Timing:
 1039 Evolutionary Preservation of Brain Rhythms. *Neuron*, *80*(3), 751–764.
 1040 <https://doi.org/10.1016/j.neuron.2013.10.002>
- 1041 Buzsáki, G., & Mizuseki, K. (2014). The log-dynamic brain: How skewed distributions affect
 1042 network operations. *Nature Reviews Neuroscience*, *15*(4), 264–278.
 1043 <https://doi.org/10.1038/nrn3687>
- 1044 Buzsáki, G., & Watson, B. O. (2012). Brain Rhythms and Neural Syntax: Implications for
 1045 Efficient Coding of Cognitive Content and Neuropsychiatric Disease. *Dialogues in*
 1046 *Clinical Neuroscience*, *14*(4), 345–367.
 1047 <https://doi.org/10.31887/DCNS.2012.14.4/gbuzsaki>
- 1048 Calin-Jageman, R. J., & Cumming, G. (2019). Estimation for Better Inference in Neuroscience.
 1049 *Eneuro*, *6*(4), ENEURO.0205-19.2019. <https://doi.org/10.1523/ENEURO.0205-19.2019>
- 1050 Caplan, J. B., Bottomley, M., Kang, P., & Dixon, R. A. (2015). Distinguishing rhythmic from non-
 1051 rhythmic brain activity during rest in healthy neurocognitive aging. *NeuroImage*, *112*,
 1052 341–352. <https://doi.org/10.1016/j.neuroimage.2015.03.001>
- 1053 Chandran KS, S., Seelamantula, C. S., & Ray, S. (2018). Duration analysis using matching
 1054 pursuit algorithm reveals longer bouts of gamma rhythm. *Journal of Neurophysiology*,
 1055 *119*(3), 808–821. <https://doi.org/10.1152/jn.00154.2017>
- 1056 Chavez, M., Besserve, M., Adam, C., & Martinerie, J. (2006). Towards a proper estimation of
 1057 phase synchronization from time series. *Journal of Neuroscience Methods*, *154*(1–2),
 1058 149–160. <https://doi.org/10.1016/j.jneumeth.2005.12.009>
- 1059 Cheveigné, A. de, & Arzounian, D. (2015). Scanning for oscillations. *Journal of Neural*
 1060 *Engineering*, *12*(6), 066020. <https://doi.org/10.1088/1741-2560/12/6/066020>
- 1061 Chiang, A. K. I., Rennie, C. J., Robinson, P. A., Roberts, J. A., Rigozzi, M. K., Whitehouse, R.
 1062 W., Hamilton, R. J., & Gordon, E. (2008). Automated characterization of multiple alpha
 1063 peaks in multi-site electroencephalograms. *Journal of Neuroscience Methods*, *168*(2),
 1064 396–411. <https://doi.org/10.1016/j.jneumeth.2007.11.001>
- 1065 Cohen, M. X. (2014). *Analyzing neural time series data: Theory and practice*. MIT Press.
- 1066 Cohen, M. X. (2017a). Rigor and replication in time-frequency analyses of cognitive
 1067 electrophysiology data. *International Journal of Psychophysiology*, *111*, 80–87.
 1068 <https://doi.org/10.1016/j.ijpsycho.2016.02.001>
- 1069 Cohen, M. X. (2017b). Comparison of linear spatial filters for identifying oscillatory activity in
 1070 multichannel data. *Journal of Neuroscience Methods*, *278*, 1–12.
 1071 <https://doi.org/10.1016/j.jneumeth.2016.12.016>
- 1072 Cohen, M. X. (2017c). Where Does EEG Come From and What Does It Mean? *Trends in*
 1073 *Neurosciences*, *40*(4), 208–218. <https://doi.org/10.1016/j.tins.2017.02.004>
- 1074 Cohen, M. X. (2021). A data-driven method to identify frequency boundaries in multichannel
 1075 electrophysiology data. *Journal of Neuroscience Methods*, *347*, 108949.
 1076 <https://doi.org/10.1016/j.jneumeth.2020.108949>
- 1077 Cohen, M. X., & Gulbinaite, R. (2014). Five methodological challenges in cognitive
 1078 electrophysiology. *NeuroImage*, *85*, 702–710.
 1079 <https://doi.org/10.1016/j.neuroimage.2013.08.010>

- 1080 Cole, S. R., Donoghue, T., Gao, R., & Voytek, B. (2019). NeuroDSP: A package for neural
 1081 digital signal processing. *Journal of Open Source Software*, 4(36), 1272.
 1082 <https://doi.org/10.21105/joss.01272>
- 1083 Cole, S. R., van der Meij, R., Peterson, E. J., de Hemptinne, C., Starr, P. A., & Voytek, B.
 1084 (2017). Nonsinusoidal Beta Oscillations Reflect Cortical Pathophysiology in Parkinson's
 1085 Disease. *The Journal of Neuroscience*, 37(18), 4830–4840.
 1086 <https://doi.org/10.1523/jneurosci.2208-16.2017>
- 1087 Cole, S. R., & Voytek, B. (2017). Brain Oscillations and the Importance of Waveform Shape.
 1088 *Trends in Cognitive Sciences*, 21(2), 137–149. <https://doi.org/10.1016/j.tics.2016.12.008>
- 1089 Cole, S. R., & Voytek, B. (2018). *Hippocampal theta bursting and waveform shape reflect CA1*
 1090 *spiking patterns* [Preprint]. bioRxiv. <https://doi.org/10.1101/452987>
- 1091 Cole, S. R., & Voytek, B. (2019). Cycle-by-cycle analysis of neural oscillations. *Journal of*
 1092 *Neurophysiology*, 122(2), 849–861. <https://doi.org/10.1152/jn.00273.2019>
- 1093 Corcoran, A. W., Alday, P. M., Schlesewsky, M., & Bornkessel-Schlesewsky, I. (2018). Toward
 1094 a reliable, automated method of individual alpha frequency (IAF) quantification.
 1095 *Psychophysiology*, 55(7), e13064. <https://doi.org/10.1111/psyp.13064>
- 1096 Cross, Z. R., Corcoran, A. W., Schlesewsky, M., Kohler, Mark. J., & Bornkessel-Schlesewsky, I.
 1097 (2020). *Oscillatory and aperiodic neural activity jointly predict grammar learning*
 1098 [Preprint]. bioRxiv. <https://doi.org/10.1101/2020.03.10.984971>
- 1099 Dähne, S., Meinecke, F. C., Haufe, S., Höhne, J., Tangermann, M., Müller, K.-R., & Nikulin, V.
 1100 V. (2014). SPoC: A novel framework for relating the amplitude of neuronal oscillations to
 1101 behaviorally relevant parameters. *NeuroImage*, 86, 111–122.
 1102 <https://doi.org/10.1016/j.neuroimage.2013.07.079>
- 1103 de Cheveigné, A., & Arzounian, D. (2018). Robust detrending, rereferencing, outlier detection,
 1104 and inpainting for multichannel data. *NeuroImage*, 172, 903–912.
 1105 <https://doi.org/10.1016/j.neuroimage.2018.01.035>
- 1106 de Cheveigné, A., & Nelken, I. (2019). Filters: When, Why, and How (Not) to Use Them.
 1107 *Neuron*, 102(2), 280–293. <https://doi.org/10.1016/j.neuron.2019.02.039>
- 1108 de Cheveigné, A., & Parra, L. C. (2014). Joint decorrelation, a versatile tool for multichannel
 1109 data analysis. *NeuroImage*, 98, 487–505.
 1110 <https://doi.org/10.1016/j.neuroimage.2014.05.068>
- 1111 Doelling, K. B., Assaneo, M. F., Bevilacqua, D., Pesaran, B., & Poeppel, D. (2019). An oscillator
 1112 model better predicts cortical entrainment to music. *Proceedings of the National*
 1113 *Academy of Sciences*, 201816414. <https://doi.org/10.1073/pnas.1816414116>
- 1114 Donoghue, T., Dominguez, J., & Voytek, B. (2020a). Electrophysiological Frequency Band Ratio
 1115 Measures Conflate Periodic and Aperiodic Neural Activity. *Eneuro*, ENEURO.0192-
 1116 20.2020. <https://doi.org/10.1523/ENEURO.0192-20.2020>
- 1117 Donoghue, T., Haller, M., Peterson, E. J., Varma, P., Sebastian, P., Gao, R., Noto, T., Lara, A.
 1118 H., Wallis, J. D., Knight, R. T., Shestyuk, A., & Voytek, B. (2020b). Parameterizing neural
 1119 power spectra into periodic and aperiodic components. *Nature Neuroscience*, 23(12),
 1120 1655–1665. <https://doi.org/10.1038/s41593-020-00744-x>
- 1121 Feingold, J., Gibson, D. J., DePasquale, B., & Graybiel, A. M. (2015). Bursts of beta oscillation
 1122 differentiate postperformance activity in the striatum and motor cortex of monkeys
 1123 performing movement tasks. *Proceedings of the National Academy of Sciences*,

- 1124 112(44), 13687–13692. <https://doi.org/10.1073/pnas.1517629112>
- 1125 Fransen, A. M. M., van Ede, F., & Maris, E. (2015). Identifying neuronal oscillations using
1126 rhythmicity. *NeuroImage*, *118*, 256–267.
1127 <https://doi.org/10.1016/j.neuroimage.2015.06.003>
- 1128 Frauscher, B., von Ellenrieder, N., Zelmann, R., Doležalová, I., Minotti, L., Olivier, A., Hall, J.,
1129 Hoffmann, D., Nguyen, D. K., Kahane, P., Dubeau, F., & Gotman, J. (2018). Atlas of the
1130 normal intracranial electroencephalogram: Neurophysiological awake activity in different
1131 cortical areas. *Brain*, *141*(4), 1130–1144. <https://doi.org/10.1093/brain/awy035>
- 1132 Freeman, W. J., Holmes, M. D., Burke, B. C., & Vanhatalo, S. (2003). Spatial spectra of scalp
1133 EEG and EMG from awake humans. *Clinical Neurophysiology*, *114*(6), 1053–1068.
1134 [https://doi.org/10.1016/S1388-2457\(03\)00045-2](https://doi.org/10.1016/S1388-2457(03)00045-2)
- 1135 Freeman, W. J., & Zhai, J. (2009). Simulated power spectral density (PSD) of background
1136 electrocorticogram (ECoG). *Cognitive Neurodynamics*, *3*(1), 97–103.
1137 <https://doi.org/10.1007/s11571-008-9064-y>
- 1138 Fries, P. (2005). A mechanism for cognitive dynamics: Neuronal communication through
1139 neuronal coherence. *Trends in Cognitive Sciences*, *9*(10), 474–480.
1140 <https://doi.org/10.1016/j.tics.2005.08.011>
- 1141 Gao, R., Peterson, E. J., & Voytek, B. (2017). Inferring synaptic excitation/inhibition balance
1142 from field potentials. *NeuroImage*, *158*, 70–78.
1143 <https://doi.org/10.1016/j.neuroimage.2017.06.078>
- 1144 Gao, R., van den Brink, R. L., Pfeffer, T., & Voytek, B. (2020). Neuronal timescales are
1145 functionally dynamic and shaped by cortical microarchitecture. *ELife*, *9*, e61277.
1146 <https://doi.org/10.7554/eLife.61277>
- 1147 Ghosh, M., Shanahan, B. E., Furtak, S. C., Mashour, G. A., Burwell, R. D., & Ahmed, O. J.
1148 (2020). Instantaneous Amplitude and Shape of Postrhinal Theta Oscillations
1149 Differentially Encode Running Speed. *Behavioral Neuroscience*, *134*(6), 516–528.
- 1150 Giehl, J., Noury, N., & Siegel, M. (2021). Dissociating harmonic and non-harmonic phase-
1151 amplitude coupling in the human brain. *NeuroImage*, *227*.
1152 <https://doi.org/10.1016/j.neuroimage.2020.117648>
- 1153 Gips, B., Bahramisharif, A., Lowet, E., Roberts, M. J., de Weerd, P., Jensen, O., & van der
1154 Eerden, J. (2017). Discovering recurring patterns in electrophysiological recordings.
1155 *Journal of Neuroscience Methods*, *275*, 66–79.
1156 <https://doi.org/10.1016/j.jneumeth.2016.11.001>
- 1157 Gleeson, P., Davison, A. P., Silver, R. A., & Ascoli, G. A. (2017). A Commitment to Open
1158 Source in Neuroscience. *Neuron*, *96*(5), 964–965.
1159 <https://doi.org/10.1016/j.neuron.2017.10.013>
- 1160 Gramfort, A. (2013). MEG and EEG data analysis with MNE-Python. *Frontiers in Neuroscience*,
1161 *7*, 267. <https://doi.org/10.3389/fnins.2013.00267>
- 1162 Grandy, T. H., Werkle-Bergner, M., Chicherio, C., Schmiedek, F., Lövdén, M., & Lindenberger,
1163 U. (2013). Peak individual alpha frequency qualifies as a stable neurophysiological trait
1164 marker in healthy younger and older adults: Alpha stability. *Psychophysiology*, *50*(6),
1165 570–582. <https://doi.org/10.1111/psyp.12043>
- 1166 Grice, J. W., Medellin, E., Jones, I., Horvath, S., McDaniel, H., O'lansen, C., & Baker, M. (2020).
1167 Persons as Effect Sizes. *Advances in Methods and Practices in Psychological Science*,

- 1168 3(4), 443–455. <https://doi.org/10.1177/2515245920922982>
- 1169 Groppe, D. M., Bickel, S., Keller, C. J., Jain, S. K., Hwang, S. T., Harden, C., & Mehta, A. D.
1170 (2013). Dominant frequencies of resting human brain activity as measured by the
1171 electrocorticogram. *NeuroImage*, 79, 223–233.
1172 <https://doi.org/10.1016/j.neuroimage.2013.04.044>
- 1173 Gross, J. (2014). Analytical methods and experimental approaches for electrophysiological
1174 studies of brain oscillations. *Journal of Neuroscience Methods*, 228, 57–66.
1175 <https://doi.org/10.1016/j.jneumeth.2014.03.007>
- 1176 Gross, J., Baillet, S., Barnes, G. R., Henson, R. N., Hillebrand, A., Jensen, O., Jerbi, K., Litvak,
1177 V., Maess, B., Oostenveld, R., Parkkonen, L., Taylor, J. R., van Wassenhove, V., Wibral,
1178 M., & Schoffelen, J.-M. (2013). Good practice for conducting and reporting MEG
1179 research. *NeuroImage*, 65, 349–363. <https://doi.org/10.1016/j.neuroimage.2012.10.001>
- 1180 Haegens, S., Cousijn, H., Wallis, G., Harrison, P. J., & Nobre, A. C. (2014). Inter- and intra-
1181 individual variability in alpha peak frequency. *NeuroImage*, 92, 46–55.
1182 <https://doi.org/10.1016/j.neuroimage.2014.01.049>
- 1183 Hari, R., & Puce, A. (2017). *MEG-EEG Primer*. Oxford University Press.
- 1184 Haufe, S., Dähne, S., & Nikulin, V. V. (2014). Dimensionality reduction for the analysis of brain
1185 oscillations. *NeuroImage*, 101, 583–597.
1186 <https://doi.org/10.1016/j.neuroimage.2014.06.073>
- 1187 Haufe, S., Meinecke, F., Görgen, K., Dähne, S., Haynes, J.-D., Blankertz, B., & Bießmann, F.
1188 (2014). On the interpretation of weight vectors of linear models in multivariate
1189 neuroimaging. *NeuroImage*, 87, 96–110.
1190 <https://doi.org/10.1016/j.neuroimage.2013.10.067>
- 1191 Haufe, S., Nikulin, V. V., Müller, K.-R., & Nolte, G. (2013). A critical assessment of connectivity
1192 measures for EEG data: A simulation study. *NeuroImage*, 64, 120–133.
1193 <https://doi.org/10.1016/j.neuroimage.2012.09.036>
- 1194 Hauk, O., Stenroos, M., & Treder, M. (2019). EEG/MEG Source Estimation and Spatial Filtering:
1195 The Linear Toolkit. In S. Supek & C. J. Aine (Eds.), *Magnetoencephalography* (pp. 1–
1196 37). Springer International Publishing. https://doi.org/10.1007/978-3-319-62657-4_85-1
- 1197 He, B. J. (2014). Scale-free brain activity: Past, present, and future. *Trends in Cognitive
1198 Sciences*, 18(9), 480–487. <https://doi.org/10.1016/j.tics.2014.04.003>
- 1199 He, W., Donoghue, T., Sowman, P. F., Seymour, R. A., Brock, J., Crain, S., Voytek, B., &
1200 Hillebrand, A. (2019). *Co-Increasing Neuronal Noise and Beta Power in the Developing
1201 Brain* (p. 49) [Preprint]. bioRxiv. <https://doi.org/10.1101/839258>
- 1202 Hindriks, R., Micheli, C., Mantini, D., & Deco, G. (2017). *Human Resting-State
1203 Electrophysiological Networks In The Alpha Frequency Band: Evidence From
1204 Magnetoencephalographic Source Imaging* [Preprint]. bioRxiv.
1205 <https://doi.org/10.1101/142091>
- 1206 Holdgraf, C., Appelhoff, S., Bickel, S., Bouchard, K., D’Ambrosio, S., David, O., Devinsky, O.,
1207 Dichter, B., Flinker, A., Foster, B. L., Gorgolewski, K. J., Groen, I., Groppe, D., Gunduz,
1208 A., Hamilton, L., Honey, C. J., Jas, M., Knight, R., Lachaux, J.-P., ... Hermes, D. (2019).
1209 IEEG-BIDS, extending the Brain Imaging Data Structure specification to human
1210 intracranial electrophysiology. *Scientific Data*, 6(1), 102. <https://doi.org/10.1038/s41597-019-0105-7>
- 1211

- 1212 Huang, Y., Parra, L. C., & Haufe, S. (2016). The New York Head—A precise standardized
 1213 volume conductor model for EEG source localization and tES targeting. *NeuroImage*,
 1214 *140*, 150–162. <https://doi.org/10.1016/j.neuroimage.2015.12.019>
- 1215 Hyvärinen, A., & Oja, E. (2000). Independent component analysis: Algorithms and applications.
 1216 *Neural Networks*, *13*(4–5), 411–430. [https://doi.org/10.1016/S0893-6080\(00\)00026-5](https://doi.org/10.1016/S0893-6080(00)00026-5)
- 1217 Jas, M., & Dupré, T. (2017). Learning the Morphology of Brain Signals Using Alpha-Stable
 1218 Convolutional Sparse Coding. *Advances in Neural Information Processing Systems*,
 1219 1099–1108.
- 1220 Jas, M., Engemann, D. A., Bekhti, Y., Raimondo, F., & Gramfort, A. (2017). Autoreject:
 1221 Automated artifact rejection for MEG and EEG data. *NeuroImage*, *159*, 417–429.
 1222 <https://doi.org/10.1016/j.neuroimage.2017.06.030>
- 1223 Jas, M., Larson, E., Engemann, D. A., Leppäkangas, J., Taulu, S., Hämäläinen, M., & Gramfort,
 1224 A. (2018). A Reproducible MEG/EEG Group Study With the MNE Software:
 1225 Recommendations, Quality Assessments, and Good Practices. *Frontiers in*
 1226 *Neuroscience*, *12*, 530. <https://doi.org/10.3389/fnins.2018.00530>
- 1227 Jones, S. R. (2016). When brain rhythms aren't 'rhythmic': Implication for their mechanisms and
 1228 meaning. *Current Opinion in Neurobiology*, *40*, 72–80.
 1229 <https://doi.org/10.1016/j.conb.2016.06.010>
- 1230 Kathawalla, U.-K., Silverstein, P., & Syed, M. (2020). *Easing Into Open Science: A Tutorial for*
 1231 *Graduate Students* [Preprint]. PsyArXiv. <https://doi.org/10.31234/osf.io/vzjdp>
- 1232 Keil, A., Debener, S., Gratton, G., Junghöfer, M., Kappenman, E. S., Luck, S. J., Luu, P., Miller,
 1233 G. A., & Yee, C. M. (2014). Committee report: Publication guidelines and
 1234 recommendations for studies using electroencephalography and
 1235 magnetoencephalography: Guidelines for EEG and MEG. *Psychophysiology*, *51*(1), 1–
 1236 21. <https://doi.org/10.1111/psyp.12147>
- 1237 Kiebel, S. J., Tallon-Baudry, C., & Friston, K. J. (2005). Parametric analysis of oscillatory activity
 1238 as measured with EEG/MEG. *Human Brain Mapping*, *26*(3), 170–177.
 1239 <https://doi.org/10.1002/hbm.20153>
- 1240 Klimesch, W. (1999). EEG alpha and theta oscillations reflect cognitive and memory
 1241 performance: A review and analysis. *Brain Research Reviews*, *29*(2), 169–195.
 1242 [https://doi.org/10.1016/S0165-0173\(98\)00056-3](https://doi.org/10.1016/S0165-0173(98)00056-3)
- 1243 Koles, Z. J. (1991). The quantitative extraction and topographic mapping of the abnormal
 1244 components in the clinical EEG. *Electroencephalography and Clinical Neurophysiology*,
 1245 *79*(6), 440–447. [https://doi.org/10.1016/0013-4694\(91\)90163-X](https://doi.org/10.1016/0013-4694(91)90163-X)
- 1246 Kosciessa, J. Q., Grandy, T. H., Garrett, D. D., & Werkle-Bergner, M. (2020). Single-trial
 1247 characterization of neural rhythms: Potential and challenges. *NeuroImage*, *206*, 116331.
 1248 <https://doi.org/10.1016/j.neuroimage.2019.116331>
- 1249 Kramer, M. A., Tort, A. B. L., & Kopell, N. J. (2008). Sharp edge artifacts and spurious coupling
 1250 in EEG frequency comodulation measures. *Journal of Neuroscience Methods*, *170*(2),
 1251 352–357. <https://doi.org/10.1016/j.jneumeth.2008.01.020>
- 1252 Krol, L. R., Pawlitzki, J., Lotte, F., Gramann, K., & Zander, T. O. (2018). SEREEGA: Simulating
 1253 event-related EEG activity. *Journal of Neuroscience Methods*, *309*, 13–24.
 1254 <https://doi.org/10.1016/j.jneumeth.2018.08.001>
- 1255 Lachaux, J.-P., Rodriguez, E., Martinerie, J., Varela, F. J., & others. (1999). Measuring phase

- 1256 synchrony in brain signals. *Human Brain Mapping*, 8(4), 194–208.
 1257 [https://doi.org/10.1002/\(SICI\)1097-0193\(1999\)8:4<194::AID-HBM4>3.0.CO;2-C](https://doi.org/10.1002/(SICI)1097-0193(1999)8:4<194::AID-HBM4>3.0.CO;2-C)
- 1258 Lakatos, P., Karmos, G., Mehta, A. D., Ulbert, I., & Schroeder, C. E. (2008). Entrainment of
 1259 Neuronal Oscillations as a Mechanism of Attentional Selection. *Science*, 320(5872),
 1260 110–113. <https://doi.org/10.1126/science.1154735>
- 1261 Lansbergen, M. M., Arns, M., van Dongen-Boomsma, M., Spronk, D., & Buitelaar, J. K. (2011).
 1262 The increase in theta/beta ratio on resting-state EEG in boys with attention-
 1263 deficit/hyperactivity disorder is mediated by slow alpha peak frequency. *Progress in*
 1264 *Neuro-Psychopharmacology and Biological Psychiatry*, 35(1), 47–52.
 1265 <https://doi.org/10.1016/j.pnpbp.2010.08.004>
- 1266 Lendner, J. D., Helfrich, R. F., Mander, B. A., Romundstad, L., Lin, J. J., Walker, M. P., Larsson,
 1267 P. G., & Knight, R. T. (2020). An electrophysiological marker of arousal level in humans.
 1268 *ELife*, 9, e55092. <https://doi.org/10.7554/eLife.55092>
- 1269 Lepage, K. Q., Kramer, M. A., & Eden, U. T. (2013). Some Sampling Properties of Common
 1270 Phase Estimators. *Neural Computation*, 25(4), 901–921.
 1271 https://doi.org/10.1162/NECO_a_00422
- 1272 Lindsley, D. B. (1939). A Longitudinal Study of the Occipital Alpha Rhythm in Normal Children:
 1273 Frequency and Amplitude Standards. *The Pedagogical Seminary and Journal of Genetic*
 1274 *Psychology*, 55(1), 197–213. <https://doi.org/10.1080/08856559.1939.10533190>
- 1275 Lopes da Silva, F. (2013). EEG and MEG: Relevance to Neuroscience. *Neuron*, 80(5), 1112–
 1276 1128. <https://doi.org/10.1016/j.neuron.2013.10.017>
- 1277 Lotte, F. & Cuntai Guan. (2011). Regularizing Common Spatial Patterns to Improve BCI
 1278 Designs: Unified Theory and New Algorithms. *IEEE Transactions on Biomedical*
 1279 *Engineering*, 58(2), 355–362. <https://doi.org/10.1109/TBME.2010.2082539>
- 1280 Lozano-Soldevilla, D., ter Huurne, N., & Oostenveld, R. (2016). Neuronal Oscillations with Non-
 1281 sinusoidal Morphology Produce Spurious Phase-to-Amplitude Coupling and
 1282 Directionality. *Frontiers in Computational Neuroscience*, 10.
 1283 <https://doi.org/10.3389/fncom.2016.00087>
- 1284 Lundqvist, M., Rose, J., Herman, P., Brincat, S. L., Buschman, T. J., & Miller, E. K. (2016).
 1285 Gamma and Beta Bursts Underlie Working Memory. *Neuron*, 90(1), 152–164.
 1286 <https://doi.org/10.1016/j.neuron.2016.02.028>
- 1287 Mahjoory, K., Nikulin, V. V., Botrel, L., Linkenkaer-Hansen, K., Fato, M. M., & Haufe, S. (2017).
 1288 Consistency of EEG source localization and connectivity estimates. *NeuroImage*, 152,
 1289 590–601. <https://doi.org/10.1016/j.neuroimage.2017.02.076>
- 1290 Mahjoory, K., Schoffelen, J.-M., Keitel, A., & Gross, J. (2020). The frequency gradient of human
 1291 resting-state brain oscillations follows cortical hierarchies. *ELife*, 9, e53715.
 1292 <https://doi.org/10.7554/eLife.53715>
- 1293 Maris, E. (2012). Statistical testing in electrophysiological studies: Statistical testing in
 1294 electrophysiological studies. *Psychophysiology*, 49(4), 549–565.
 1295 <https://doi.org/10.1111/j.1469-8986.2011.01320.x>
- 1296 Maris, E., & Oostenveld, R. (2007). Nonparametric statistical testing of EEG- and MEG-data.
 1297 *Journal of Neuroscience Methods*, 164(1), 177–190.
 1298 <https://doi.org/10.1016/j.jneumeth.2007.03.024>
- 1299 Mazaheri, A., Slagter, H. A., Thut, G., & Foxe, J. J. (2018). Orchestration of brain oscillations:

- 1300 Principles and functions. *European Journal of Neuroscience*, 48(7), 2385–2388.
 1301 <https://doi.org/10.1111/ejn.14189>
- 1302 Miller, E. K., Lundqvist, M., & Bastos, A. M. (2018). Working Memory 2.0. *Neuron*, 100(2), 463–
 1303 475. <https://doi.org/10.1016/j.neuron.2018.09.023>
- 1304 Miller, K. J., Honey, C. J., Hermes, D., Rao, R. P., den Nijs, M., & Ojemann, J. G. (2014).
 1305 Broadband changes in the cortical surface potential track activation of functionally
 1306 diverse neuronal populations. *NeuroImage*, 85, 711–720.
 1307 <https://doi.org/10.1016/j.neuroimage.2013.08.070>
- 1308 Miller, K. J., Sorensen, L. B., Ojemann, J. G., & den Nijs, M. (2009). Power-Law Scaling in the
 1309 Brain Surface Electric Potential. *PLOS Computational Biology*, 5(12), e1000609.
 1310 <https://doi.org/10.1371/journal.pcbi.1000609>
- 1311 Mortezapouraghdam, Z., Corona-Strauss, F. I., Takahashi, K., & Strauss, D. J. (2018).
 1312 Reducing the Effect of Spurious Phase Variations in Neural Oscillatory Signals. *Frontiers*
 1313 *in Computational Neuroscience*, 12, 82. <https://doi.org/10.3389/fncom.2018.00082>
- 1314 Muthukumaraswamy, S. D., & Singh, K. D. (2011). A cautionary note on the interpretation of
 1315 phase-locking estimates with concurrent changes in power. *Clinical Neurophysiology*,
 1316 122(11), 2324–2325. <https://doi.org/10.1016/j.clinph.2011.04.003>
- 1317 Newson, J. J., & Thiagarajan, T. C. (2019). EEG Frequency Bands in Psychiatric Disorders: A
 1318 Review of Resting State Studies. *Frontiers in Human Neuroscience*, 12.
 1319 <https://doi.org/10.3389/fnhum.2018.00521>
- 1320 Neymotin, S. A., Barczak, A., O'Connell, M. N., McGinnis, T., Markowitz, N., Espinal, E., Griffith,
 1321 E., Anwar, H., Dura-Bernal, S., Lytton, W. W., Jones, S. R., Bickel, S., & Lakatos, P.
 1322 (2020). *Taxonomy of neural oscillation events in primate auditory cortex* [Preprint].
 1323 bioRxiv. <https://doi.org/10.1101/2020.04.16.045021>
- 1324 Neymotin, S. A., Daniels, D. S., Caldwell, B., McDougal, R. A., Carnevale, N. T., Jas, M.,
 1325 Moore, C. I., Hines, M. L., Hämäläinen, M., & Jones, S. R. (2020). Human Neocortical
 1326 Neurosolver (HNN), a new software tool for interpreting the cellular and network origin of
 1327 human MEG/EEG data. *eLife*, 9, e51214. <https://doi.org/10.7554/eLife.51214>
- 1328 Nikulin, V. V., Nolte, G., & Curio, G. (2011). A novel method for reliable and fast extraction of
 1329 neuronal EEG/MEG oscillations on the basis of spatio-spectral decomposition.
 1330 *NeuroImage*, 55(4), 1528–1535. <https://doi.org/10.1016/j.neuroimage.2011.01.057>
- 1331 Niso, G., Gorgolewski, K. J., Bock, E., Brooks, T. L., Flandin, G., Gramfort, A., Henson, R. N.,
 1332 Jas, M., Litvak, V., T. Moreau, J., Oostenveld, R., Schoffelen, J.-M., Tadel, F., Wexler,
 1333 J., & Baillet, S. (2018). MEG-BIDS, the brain imaging data structure extended to
 1334 magnetoencephalography. *Scientific Data*, 5(1), 180110.
 1335 <https://doi.org/10.1038/sdata.2018.110>
- 1336 Nunez, P. L., & Srinivasan, R. (2006). *Electric fields of the brain: The neurophysics of EEG* (2nd
 1337 ed). Oxford University Press.
- 1338 O'Neill, G. C., Tewarie, P., Vidaurre, D., Liuzzi, L., Woolrich, M. W., & Brookes, M. J. (2018).
 1339 Dynamics of large-scale electrophysiological networks: A technical review. *NeuroImage*,
 1340 180, 559–576. <https://doi.org/10.1016/j.neuroimage.2017.10.003>
- 1341 Oostenveld, R., Fries, P., Maris, E., & Schoffelen, J.-M. (2011). FieldTrip: Open Source
 1342 Software for Advanced Analysis of MEG, EEG, and Invasive Electrophysiological Data.
 1343 *Computational Intelligence and Neuroscience*, 2011, 1–9.

- 1344 <https://doi.org/10.1155/2011/156869>
- 1345 Palva, J. M., Wang, S. H., Palva, S., Zhigalov, A., Monto, S., Brookes, M. J., Schoffelen, J.-M.,
1346 & Jerbi, K. (2018). Ghost interactions in MEG/EEG source space: A note of caution on
1347 inter-areal coupling measures. *NeuroImage*, *173*, 632–643.
1348 <https://doi.org/10.1016/j.neuroimage.2018.02.032>
- 1349 Palva, S., & Palva, J. M. (2012). Discovering oscillatory interaction networks with M/EEG:
1350 Challenges and breakthroughs. *Trends in Cognitive Sciences*, *16*(4), 219–230.
1351 <https://doi.org/10.1016/j.tics.2012.02.004>
- 1352 Parra, L. C., Spence, C. D., Gerson, A. D., & Sajda, P. (2005). Recipes for the linear analysis of
1353 EEG. *NeuroImage*, *28*(2), 326–341. <https://doi.org/10.1016/j.neuroimage.2005.05.032>
- 1354 Pascual-Marqui, R. D., Valdes-Sosa, P. A., & Alvarez-Amador, A. (1988). A Parametric Model
1355 for Multichannel EEG Spectra. *International Journal of Neuroscience*, *40*(1–2), 89–99.
1356 <https://doi.org/10.3109/00207458808985730>
- 1357 Pernet, C. R., Appelhoff, S., Gorgolewski, K. J., Flandin, G., Phillips, C., Delorme, A., &
1358 Oostenveld, R. (2019). EEG-BIDS, an extension to the brain imaging data structure for
1359 electroencephalography. *Scientific Data*, *6*(1), 103. <https://doi.org/10.1038/s41597-019-0104-8>
- 1360
- 1361 Pernet, C. R., Garrido, M. I., Gramfort, A., Maurits, N., Michel, C. M., Pang, E., Salmelin, R.,
1362 Schoffelen, J. M., Valdes-Sosa, P. A., & Puce, A. (2020). Issues and recommendations
1363 from the OHBM COBIDAS MEEG committee for reproducible EEG and MEG research.
1364 *Nature Neuroscience*, *23*(12), 1473–1483. <https://doi.org/10.1038/s41593-020-00709-0>
- 1365 Pesaran, B., Vinck, M., Einevoll, G. T., Sirota, A., Fries, P., Siegel, M., Truccolo, W., Schroeder,
1366 C. E., & Srinivasan, R. (2018). Investigating large-scale brain dynamics using field
1367 potential recordings: Analysis and interpretation. *Nature Neuroscience*.
1368 <https://doi.org/10.1038/s41593-018-0171-8>
- 1369 Pfurtscheller, G., & Lopes da Silva, F. H. (1999). Event-related EEG/MEG synchronization and
1370 desynchronization: Basic principles. *Clinical Neurophysiology*, *110*(11), 1842–1857.
1371 [https://doi.org/10.1016/S1388-2457\(99\)00141-8](https://doi.org/10.1016/S1388-2457(99)00141-8)
- 1372 Piastra, M. C., Nüßing, A., Vorwerk, J., Clerc, M., Engwer, C., & Wolters, C. H. (2020). A
1373 comprehensive study on electroencephalography and magnetoencephalography
1374 sensitivity to cortical and subcortical sources. *Human Brain Mapping*, *hbm.25272*.
1375 <https://doi.org/10.1002/hbm.25272>
- 1376 Podvalny, E., Noy, N., Harel, M., Bickel, S., Chechik, G., Schroeder, C. E., Mehta, A. D.,
1377 Tsodyks, M., & Malach, R. (2015). A unifying principle underlying the extracellular field
1378 potential spectral responses in the human cortex. *Journal of Neurophysiology*, *114*(1),
1379 505–519. <https://doi.org/10.1152/jn.00943.2014>
- 1380 Popov, T., Oostenveld, R., & Schoffelen, J. M. (2018). FieldTrip Made Easy: An Analysis
1381 Protocol for Group Analysis of the Auditory Steady State Brain Response in Time,
1382 Frequency, and Space. *Frontiers in Neuroscience*, *12*, 711.
1383 <https://doi.org/10.3389/fnins.2018.00711>
- 1384 Quinn, A. J., van Ede, F., Brookes, M. J., Heideman, S. G., Nowak, M., Seedat, Z. A., Vidaurre,
1385 D., Zich, C., Nobre, A. C., & Woolrich, M. W. (2019). Unpacking Transient Event
1386 Dynamics in Electrophysiological Power Spectra. *Brain Topography*, *32*, 1020–1034.
1387 <https://doi.org/10.1007/s10548-019-00745-5>

- 1388 Rey, H. G., Ahmadi, M., & Quian Quiroga, R. (2015). Single trial analysis of field potentials in
 1389 perception, learning and memory. *Current Opinion in Neurobiology*, *31*, 148–155.
 1390 <https://doi.org/10.1016/j.conb.2014.10.009>
- 1391 Robertson, M. M., Furlong, S., Voytek, B., Donoghue, T., Boettiger, C. A., & Sheridan, M. A.
 1392 (2019). EEG Power Spectral Slope differs by ADHD status and stimulant medication
 1393 exposure in early childhood. *Journal of Neurophysiology*, *122*(6), 2427–2437.
 1394 <https://doi.org/10.1152/jn.00388.2019>
- 1395 Sameni, R., & Seraj, E. (2017). A robust statistical framework for instantaneous
 1396 electroencephalogram phase and frequency estimation and analysis. *Physiological
 1397 Measurement*, *38*(12), 2141–2163. <https://doi.org/10.1088/1361-6579/aa93a1>
- 1398 Sanz Leon, P., Knock, S. A., Woodman, M. M., Domide, L., Mersmann, J., McIntosh, A. R., &
 1399 Jirsa, V. (2013). The Virtual Brain: A simulator of primate brain network dynamics.
 1400 *Frontiers in Neuroinformatics*, *7*. <https://doi.org/10.3389/fninf.2013.00010>
- 1401 Schaworonkow, N., Blythe, D. A. J., Kegeles, J., Curio, G., & Nikulin, V. V. (2015). Power-law
 1402 dynamics in neuronal and behavioral data introduce spurious correlations: Power-Law
 1403 Dynamics in Neuronal and Behavioral Data. *Human Brain Mapping*, *36*(8), 2901–2914.
 1404 <https://doi.org/10.1002/hbm.22816>
- 1405 Schaworonkow, N., & Nikulin, V. V. (2019). Spatial neuronal synchronization and the waveform
 1406 of oscillations: Implications for EEG and MEG. *PLOS Computational Biology*, *15*(5),
 1407 e1007055. <https://doi.org/10.1371/journal.pcbi.1007055>
- 1408 Schoffelen, J.-M., & Gross, J. (2009). Source connectivity analysis with MEG and EEG. *Human
 1409 Brain Mapping*, *30*(6), 1857–1865. <https://doi.org/10.1002/hbm.20745>
- 1410 Sherman, M. A., Lee, S., Law, R., Haegens, S., Thorn, C. A., Hamalainen, M. S., Moore, C. I., &
 1411 Jones, S. R. (2016). Neural mechanisms of transient neocortical beta rhythms:
 1412 Converging evidence from humans, computational modeling, monkeys, and mice.
 1413 *Proceedings of the National Academy of Sciences*, *113*(33), E4885–E4894.
 1414 <https://doi.org/10.1073/pnas.1604135113>
- 1415 Shin, H., Law, R., Tsutsui, S., Moore, C. I., & Jones, S. R. (2017). The rate of transient beta
 1416 frequency events predicts behavior across tasks and species. *ELife*, *6*, e29086.
 1417 <https://doi.org/10.7554/eLife.29086>
- 1418 Stokes, M., & Spaak, E. (2016). The Importance of Single-Trial Analyses in Cognitive
 1419 Neuroscience. *Trends in Cognitive Sciences*, *20*(7), 483–486.
 1420 <https://doi.org/10.1016/j.tics.2016.05.008>
- 1421 Timmer, J., & Konig, M. (1995). On Generating Power Law Noise. *Astronomy and Astrophysics*,
 1422 *300*, 707–710.
- 1423 Urigüen, J. A., & Garcia-Zapirain, B. (2015). EEG artifact removal—State-of-the-art and
 1424 guidelines. *Journal of Neural Engineering*, *12*(3), 031001. <https://doi.org/10.1088/1741-2560/12/3/031001>
- 1425
- 1426 van Diepen, R. M., & Mazaheri, A. (2018). The Caveats of observing Inter-Trial Phase-
 1427 Coherence in Cognitive Neuroscience. *Scientific Reports*, *8*(1).
 1428 <https://doi.org/10.1038/s41598-018-20423-z>
- 1429 van Ede, F., Quinn, A. J., Woolrich, M. W., & Nobre, A. C. (2018). Neural Oscillations:
 1430 Sustained Rhythms or Transient Burst-Events? *Trends in Neurosciences*, *41*(7), 415–
 1431 417. <https://doi.org/10.1016/j.tins.2018.04.004>

- 1432 van Vugt, M. K., Sederberg, P. B., & Kahana, M. J. (2007). Comparison of spectral analysis
 1433 methods for characterizing brain oscillations. *Journal of Neuroscience Methods*, 162(1–
 1434 2), 49–63. <https://doi.org/10.1016/j.jneumeth.2006.12.004>
- 1435 VanRullen, R. (2016). Perceptual Cycles. *Trends in Cognitive Sciences*, 20(10), 723–735.
 1436 <https://doi.org/10.1016/j.tics.2016.07.006>
- 1437 Varela, F. J., Lachaux, J.-P., Rodriguez, E., & Martinerie, J. (2001). The brainweb: Phase
 1438 synchronization and large-scale integration. *Nature Reviews Neuroscience*, 2(4), 229–
 1439 239. <https://doi.org/10.1038/35067550>
- 1440 Vaz, A. P., Yaffe, R. B., Wittig, J. H., Inati, S. K., & Zaghloul, K. A. (2017). Dual origins of
 1441 measured phase-amplitude coupling reveal distinct neural mechanisms underlying
 1442 episodic memory in the human cortex. *NeuroImage*, 148, 148–159.
 1443 <https://doi.org/10.1016/j.neuroimage.2017.01.001>
- 1444 Vidaurre, D., Quinn, A. J., Baker, A. P., Dupret, D., Tejero-Cantero, A., & Woolrich, M. W.
 1445 (2016). Spectrally resolved fast transient brain states in electrophysiological data.
 1446 *NeuroImage*, 126, 81–95. <https://doi.org/10.1016/j.neuroimage.2015.11.047>
- 1447 Voytek, B. (2016). The Virtuous Cycle of a Data Ecosystem. *PLOS Computational Biology*,
 1448 12(8), e1005037. <https://doi.org/10.1371/journal.pcbi.1005037>
- 1449 Voytek, B., & Knight, R. T. (2015). Dynamic Network Communication as a Unifying Neural Basis
 1450 for Cognition, Development, Aging, and Disease. *Biological Psychiatry*, 77(12), 1089–
 1451 1097. <https://doi.org/10.1016/j.biopsych.2015.04.016>
- 1452 Voytek, B., Kramer, M. A., Case, J., Lepage, K. Q., Tempesta, Z. R., Knight, R. T., & Gazzaley,
 1453 A. (2015). Age-Related Changes in 1/f Neural Electrophysiological Noise. *Journal of*
 1454 *Neuroscience*, 35(38), 13257–13265. <https://doi.org/10.1523/JNEUROSCI.2332-14.2015>
- 1455 Wacker, M., & Witte, H. (2013). Time-frequency Techniques in Biomedical Signal Analysis: A
 1456 Tutorial Review of Similarities and Differences. *Methods of Information in Medicine*,
 1457 52(04), 279–296. <https://doi.org/10.3414/ME12-01-0083>
- 1458 Wang, X.-J. (2010). Neurophysiological and Computational Principles of Cortical Rhythms in
 1459 Cognition. *Physiological Reviews*, 90(3), 1195–1268.
 1460 <https://doi.org/10.1152/physrev.00035.2008>
- 1461 Waschke, L., Donoghue, T., Fiedler, L., Smith, S., Voytek, B., & Obleser, J. (2021). *Modality-*
 1462 *specific tracking of attention and sensory statistics in the human electrophysiological*
 1463 *spectral exponent* [Preprint]. bioRxiv. <https://doi.org/10.1101/2021.01.13.426522>
- 1464 Watrous, A. J., & Buchanan, R. J. (2020). The Oscillatory ReConstruction Algorithm adaptively
 1465 identifies frequency bands to improve spectral decomposition in human and rodent
 1466 neural recordings. *Journal of Neurophysiology*, 124(6), 1914–1922.
 1467 <https://doi.org/10.1152/jn.00292.2020>
- 1468 Watrous, A. J., Miller, J., Qasim, S. E., Fried, I., & Jacobs, J. (2018). Phase-tuned neuronal
 1469 firing encodes human contextual representations for navigational goals. *ELife*, 7,
 1470 e32554. <https://doi.org/10.7554/eLife.32554>
- 1471 Wen, H., & Liu, Z. (2016). Separating Fractal and Oscillatory Components in the Power
 1472 Spectrum of Neurophysiological Signal. *Brain Topography*, 29(1), 13–26.
 1473 <https://doi.org/10.1007/s10548-015-0448-0>
- 1474 Wessel, J. R. (2020). β -Bursts Reveal the Trial-to-Trial Dynamics of Movement Initiation and
 1475 Cancellation. *The Journal of Neuroscience*, 40(2), 411–423.

- 1476 <https://doi.org/10.1523/JNEUROSCI.1887-19.2019>
- 1477 Whitten, T. A., Hughes, A. M., Dickson, C. T., & Caplan, J. B. (2011). A better oscillation
1478 detection method robustly extracts EEG rhythms across brain state changes: The
1479 human alpha rhythm as a test case. *NeuroImage*, *54*(2), 860–874.
1480 <https://doi.org/10.1016/j.neuroimage.2010.08.064>
- 1481 Widmann, A., Schröger, E., & Maess, B. (2015). Digital filter design for electrophysiological data
1482 – a practical approach. *Journal of Neuroscience Methods*, *250*, 34–46.
1483 <https://doi.org/10.1016/j.jneumeth.2014.08.002>
- 1484 Wilson, G., Bryan, J., Cranston, K., Kitzes, J., Nederbragt, L., & Teal, T. K. (2017). Good
1485 enough practices in scientific computing. *PLOS Computational Biology*, *13*(6),
1486 e1005510. <https://doi.org/10.1371/journal.pcbi.1005510>
- 1487 Wutz, A., Melcher, D., & Samaha, J. (2018). Frequency modulation of neural oscillations
1488 according to visual task demands. *Proceedings of the National Academy of Sciences*,
1489 *115*(6), 1346–1351. <https://doi.org/10.1073/pnas.1713318115>
- 1490 Zich, C., Quinn, A. J., Mardell, L. C., Ward, N. S., & Bestmann, S. (2020). Dissecting Transient
1491 Burst Events. *Trends in Cognitive Sciences*, *24*(10), 784–788.
1492 <https://doi.org/10.1016/j.tics.2020.07.004>
- 1493